

Turbulence: A Nonequilibrium Field Theory

Mahendra Verma^{1*}

^{1*}Department of Physics, Indian Institute of Technology Kanpur,
Kanpur, 208016, UP, India.

Corresponding author(s). E-mail(s): mkv@iitk.ac.in;

Abstract

Tools of quantum and statistical field theories have been successfully ported to turbulence. Here, we review the key results of turbulence field theory. *Equilibrium field theory* describes thermalized spectrally-truncated Euler equation, where the equipartitioned Fourier modes generate zero energy flux. In contrast, *nonequilibrium field theory* is employed for modelling of hydrodynamic turbulence (HDT), which has small viscosity. In HDT, viscosity renormalization yields wavenumber-dependent viscosity and energy spectrum. Field theory calculations also yields nonzero energy flux for HDT. These field theory computations have been generalized to other systems, e.g., passive scalar and magnetohydrodynamics. In this review, I cover these aspects, along with a brief coverage of weak turbulence and intermittency.

Keywords: Hydrodynamic Turbulence, Field theory, Renormalization Group, Energy Transfers and Flux, Weak Turbulence

1 Introduction

Classical and quantum field theories are critical pillars of modern physics, and they successfully explain complex many-body systems in high-energy, condensed-matter, and statistical physics [1–3]. Notable results of field theory are the running coupling constants in quantum electrodynamics (QED) and quantum chromodynamics (QCD) [1]; universality in second-order phase transition [4]; quantum Hall effect; and turbulence, a topic of the present review.

Early applications of quantum field theories were for equilibrium systems, e.g., Ising Hamiltonian, free-electron theory, ϕ^4 theory, and Hubbard model. Here, the

fields are in equilibrium, which leads to the energy spectrum $E(k) \sim k^{d-1}$ in d dimensions [2, 3]. Analogous equilibrium system in hydrodynamics is spectrally-truncated Euler equation [5].

Note, however, that many physical systems, including turbulence, are out of equilibrium. Such systems are often forced and dissipative at different length scales, leading to uneven energy distribution across scales. For example, the energy spectrum for three-dimensional (3D) hydrodynamic turbulence (HDT) is $k^{-5/3}$, not equilibrium k^{d-1} . [6–8] In addition, nonequilibrium systems often exhibit multiscale energy cascades, which are absent in equilibrium systems. In this review, we will contrast the equilibrium and nonequilibrium properties of turbulent flows.

Another common feature among field theory calculations is *Perturbative expansion* [1–3]. Here, the contributions of the nonlinear or interaction term are computed perturbatively over the linear term. The relative strength of the interaction term over the linear term is called the *coupling constant* of the theory. QED, conventional superconductors, weakly interacting Bose gases, and many other quantum systems have small coupling constants. Hence, perturbation expansion is justified for such systems. In contrast, perturbative expansion is not employed to QCD because its the coupling constant is larger than unity. Interestingly, the coupling constant of HDT is of the order of unity. Yet, perturbative turbulence field theory yields reasonable results, which will be discussed in this review.

Nonequilibrium nature of turbulence makes its field theory interesting, as well as challenging with several unsolved problems. In this paper, I will review important developments in field theory of turbulence. There are many books [9–12] and review articles [13–19] on this topic. Hence, for novelty, this review attempts to bring in new perspectives and presents a couple of new results. For example, I contrast turbulence field theory with equilibrium field theories, and present new and unpublished field-theoretic calculations on passive scalar and magnetohydrodynamic turbulence based on Craya-Herring basis.

After these introductory remarks, I introduce some key results of turbulence field theory, whose starting point is *incompressible Navier-Stokes equations*:

$$\frac{\partial \mathbf{u}}{\partial t} - \nu \nabla^2 \mathbf{u} = -\lambda \mathbf{u} \cdot \nabla \mathbf{u} - \nabla p + \mathbf{f}, \quad (1)$$

$$\nabla \cdot \mathbf{u} = 0, \quad (2)$$

where \mathbf{u} , p are the velocity and pressure fields, respectively; λ is the coupling constant; ν is the kinematic viscosity; and \mathbf{f} is the coloured noise with the following correlation:

$$\langle f_i(\mathbf{x}) f_l(\mathbf{x}') \rangle \sim |\mathbf{x} - \mathbf{x}'|^{y-d-z}, \quad (3)$$

where d is the space dimension; y is the exponent for the spatial force-force correlation; and z is the dynamic exponent ($\omega \sim k^z$, where ω is frequency).

Equations (1, 2) do not have a general mathematical solution. In fact, it is not yet known if Eqs. (1, 2) admit a smooth solution for small viscosity [20]. Fortunately, stalwarts like Taylor, Batchelor, Kolmogorov, Chandrasekhar, and others solved for the Green's and correlation functions under the assumption of homogeneity and isotropy.

For brevity, we present only the Kolmogorov’s K41 theory, according to which, for large-scale forcing with $\nu \rightarrow 0$, under the assumption of homogeneity and isotropy, the third-order structure function is [6, 7, 20]

$$S_3(l) = \left\langle |(\mathbf{u}(\mathbf{x} + \mathbf{l}) - \mathbf{u}(\mathbf{x})) \cdot \hat{l}|^3 \right\rangle = -\frac{4}{5}\Pi l, \quad (4)$$

where \hat{l} is unit vector along \mathbf{l} , and Π is the energy flux in the inertial range. Using Eq. (4), it is easy to derive the energy spectrum for HDT as $k^{-5/3}$. We may call K41 theory as a field theory, with Eq. (4) as an exact field-theoretic relation. However, this calculation differs from ones using standard perturbative method. Kraichnan pioneered turbulence field theory, starting with his influential paper on *direct interaction approximation* (DIA).

Kraichnan [21] employed DIA, a first-order perturbative field theory, to HDT and derived the equations for the Green’s and correlations functions. The integral for the Green’s function (*self-energy integral*) diverges at small wavenumbers, which called the *infrared divergence* problem in field theory. To cure this problem, Kraichnan [21] introduced an infrared cutoff for the integral. But, this trick leads to $k^{-3/2}$ energy spectrum the contradicts observed $k^{-5/3}$ energy spectrum for HDT. We will discuss Kraichnan’s formalism in Section 3. Later, Kraichnan performed more complex field theory computations—*Mixed Lagrangian-Eulerian approach* [22], *Lagrangian-History Closure Approximation* [23], *Test Field Model* [24]—to derive $k^{-5/3}$ energy spectrum for HDT. Another important field theory work on turbulence is by Wyld [25] who wrote Feynman diagrams to higher orders. Unfortunately, Wyld did not close the equations to predict the Green’s and correlation functions for HDT.

Renormalization groups (RG) provides a pathway to solve the infrared divergence problem. Yakhot and Orszag [26] and Forster et al. [27] applied RG to hydrodynamic turbulence and derived interesting results. For example, Yakhot and Orszag [26] obtained Kolmogorov’s $k^{-5/3}$ energy spectrum for $y = d$ [see Eq. (3)]. McComb [10], McComb and Watt [28], and Zhou et al. [29] employed recursive self-consistent RG and showed that the renormalized viscosity scales as $k^{-4/3}$, and that the energy spectrum scales as $k^{-5/3}$. We will discuss these theories in Sections 4.1 and 4.2.

Kraichnan [21], Yakhot and Orszag [26], Forster et al. [27], McComb and Watt [28], and Zhou et al. [29] employed perturbative expansion to the Navier-Stokes equation. This is in contrast to standard field-theory practice of using Hamiltonian, Lagrangian, or generating functionals. Note, however, that DeDominicis and Martin [30] and Martin et al. [31] constructed generating functionals for HDT using coloured noise or forcing [Eq. (3)]. DeDominicis and Martin [30] derived a relationship between the Green’s function and correlation function using Callan-Symanzik equation, and Kolmogorov’s spectrum for a special case of forcing.

Field-theoretic computations are quite tedious involving complex tensor algebra. Recently, Verma [32] employed Craya-Herring basis that simplified the calculations tremendously. In this framework, pressure is eliminated automatically. More importantly, each Craya-Herring component of the velocity field has its own renormalized viscosity. I will cover these results in Section 4.3. Turbulence is a dynamic phenomena with nonzero multiscale energy transfers. Fortunately, turbulence energy transfers have

been computed using first-order perturbation, starting from Kraichnan [21]. I will discuss these computations in Section 5. In addition, I will discuss field theories of scalar and magnetohydrodynamic (MHD) turbulence in Sections 6 and 7; Craya-Herring basis simplifies these computations significantly and provide interesting relationships with HDT.

Now, I discuss some topics they are not detailed in this review. Many real flows involve gravitational field, or magnetic field, or some other external fields that make the flow anisotropic. Anisotropic field theories are quite complex and they are beyond the scope of this review. In addition, I do not delve into the first-principle derivation of multipoint correlation functions, a topic related to intermittency [33, 34]. In another front, weak turbulence theory employs field-theoretic tools with nonlinear term as a small perturbation over the linear term. In Sections 8 and 9, I will discuss weak turbulence and intermittency very briefly. In Section 10, I compare and contrast various field theories including turbulence.

The present review employs many symbols; I tabulate them in Table 1 for convenience of the reader. In the following section, I will introduce the basic equations used in this review.

Table 1 Abbreviation and symbols used in this review.

Symbol	Stands for	Symbol	Stands for
CH	Craya-Herring	HDT	Hydrodynamic turbulence
KE	Kinetic energy	ME	Magnetic energy
RG	Renormalization group	NS	Navier-Stokes
MHD	Magnetohydrodynamics	$c = k_{n+1}/k_n$	wavenumber binning parameter
\mathbf{r}	space coordinate	\mathbf{k}	wavenumber
\mathbf{u}	velocity field	u_1	CH basis: 1st component
d	space dimension	u_2	CH basis: 2nd component
\mathbf{f}	force field to \mathbf{u}	ψ	Scalar field
\mathbf{b}	magnetic field	$\mathbf{z}^\pm = \mathbf{u} \pm \mathbf{b}$	Elsässer variables
$E(k)$	1D KE spectrum	$E(\mathbf{k}) = \frac{1}{2} \mathbf{u}(\mathbf{k}) ^2$	Modal KE
$ u_1(\mathbf{k}) ^2 = C_1(\mathbf{k})$	Spectral correlation for $u_1(\mathbf{k})$	$ u_2(\mathbf{k}) ^2 = C_2(\mathbf{k})$	Spectral correlation for $u_2(\mathbf{k})$
$C_1(\mathbf{k}) = C_2(\mathbf{k})$	$C(\mathbf{k})$ (isotropy)	$G(\mathbf{k})$	Green's function for \mathbf{u}
$G_1(\mathbf{k})$	Green's function for u_1	$G_2(\mathbf{k})$	Green's function for u_2
$ \psi(\mathbf{k}) ^2 = C^\psi(\mathbf{k})$	Spectral correlation for $\psi(\mathbf{k})$	$G^\psi(\mathbf{k})$	Green's function for ψ
$\bar{C}_{1,2}(\mathbf{k}, t - t')$	two-time correlation functions for $u_{1,2}$	$\bar{C}^\psi(\mathbf{k}, t - t')$	two-time correlation function for ψ
$\bar{C}_{1,2}^\pm(\mathbf{k}, t - t')$	two-time correlation functions for $z_{1,2}^\pm$	$G_{1,2}^\pm(\mathbf{k}, t - t')$	Green's function for $z_{1,2}^\pm$
K_{Ko}	Kolmogorov constant	K_ψ	Obukhov-Corrsion constant
K^\pm	Kolmogorov constant for \mathbf{z}^\pm	ν_1	viscosity for u_1
ν	Kinematic viscosity	$\nu_{1,2*}$	RG constant for $\nu_{1,2}$
ν_2	viscosity for u_2	κ_*	RG constant for κ
κ	Scalar diffusivity	η_\pm	$(\nu \pm \eta)/2$
η	magnetic diffusivity	$\eta_{1,2*}$	RG constants for $\eta_{1,2}$
$\eta_{1,2}$	diffusivities for $(z^\pm)_{1,2}$ [$\langle z^+ ^2 \rangle = \langle z^- ^2 \rangle$]	Π_ψ	Energy flux for ψ
Π	Energy flux for \mathbf{u}	Π_{u_2}	Energy flux of u_2
Π_{u_1}	Energy flux of u_1	Π_{z_2}	Energy flux of z_2 ($E^+ = E^-$)
Π_{z_1}	Energy flux of z_1		

2 Governing Equations

Field-theoretic methods often employ spatial and temporal averaging, which is sensible for homogeneous and isotropic systems. In addition, the system is assumed to be steady that leads to two-time temporal correlations and Green's functions being independent of absolute time, that is, $F(t, t') = F(t - t')$ for any function F . This framework has been adopted in turbulence field theory. Most field-theoretic works on turbulence are for incompressible hydrodynamics, which is described using incompressible Navier-Stokes (NS) equations [Eqs. (1, 2)]. In the following discussion, we present the equations employed in field-theoretic calculations.

2.1 Incompressible Navier-Stokes Equation

Field-theoretic calculations are often performed in Fourier space, where the equations for the incompressible Navier-Stokes equations are [8, 35]

$$(\partial_t + \nu k^2) \mathbf{u}(\mathbf{k}, t) = -i\lambda \int \frac{d\mathbf{p}}{(2\pi)^d} \{\mathbf{k} \cdot \mathbf{u}(\mathbf{q}, t)\} \mathbf{u}(\mathbf{p}, t) - i\mathbf{k}p(\mathbf{k}, t) + \mathbf{f}(\mathbf{k}, t), \quad (5)$$

$$\mathbf{k} \cdot \mathbf{u}(\mathbf{k}, t) = 0. \quad (6)$$

Here, $\mathbf{k} = \mathbf{p} + \mathbf{q}$; λ is the coupling constant; d is the space dimension; and ν is kinematic viscosity. The transformations from real space to Fourier space and vice versa are as follows [1]:

$$\mathbf{u}(\mathbf{r}, t) = \int \frac{d\mathbf{k}}{(2\pi)^d} \mathbf{u}(\mathbf{k}, t) \exp(i\mathbf{k} \cdot \mathbf{r}); \quad \mathbf{u}(\mathbf{k}, t) = \int d\mathbf{r} [\mathbf{u}(\mathbf{r}, t) \exp(-i\mathbf{k} \cdot \mathbf{r})], \quad (7)$$

and the pressure field is determined using the following equation [8]:

$$p(\mathbf{k}, t) = -\frac{\lambda}{k^2} \int \frac{d\mathbf{p}}{(2\pi)^d} \{\mathbf{k} \cdot \mathbf{u}(\mathbf{q}, t)\} \{\mathbf{k} \cdot \mathbf{u}(\mathbf{p}, t)\}, \quad (8)$$

with $\mathbf{k} \cdot \mathbf{f}(\mathbf{k}, t) = 0$. *Galilean invariance* of NS equation leads to $\lambda = 1$ [27]; this result plays a critical role in turbulence field theory.

Many field-theoretic calculations have been performed in frequency and wavenumber space, where the NS equations in tensorial form are [9, 21]

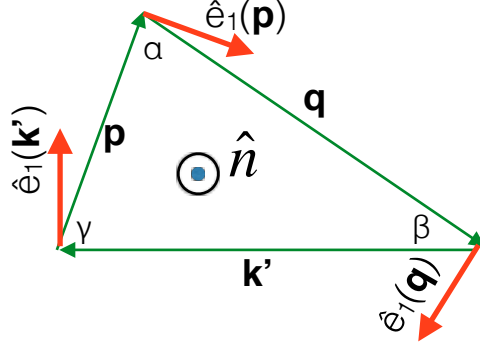
$$(-i\omega + \nu k^2) u_l(\hat{k}) = -i\frac{\lambda}{2} P_{lmn}(\mathbf{k}) \int_{\hat{p}+\hat{q}=\hat{k}} d\hat{p} [u_m(\hat{q})u_n(\hat{p})] + f_l(\hat{k}), \quad (9)$$

$$k_l u_l(\hat{k}) = 0, \quad (10)$$

where ω is the frequency, $\hat{k} = (\mathbf{k}, \omega)$, $\hat{p} + \hat{q} = \hat{k}$, and

$$P_{lmn}(\mathbf{k}) = k_m P_{lm}(\mathbf{k}) + k_n P_{lm}(\mathbf{k}), \quad (11)$$

$$P_{lm}(\mathbf{k}) = \delta_{lm} - \frac{k_l k_m}{k^2}, \quad (12)$$



$$\hat{e}_2(\mathbf{k}') = \hat{e}_2(\mathbf{p}) = \hat{e}_2(\mathbf{q}) = -\hat{n}$$

Fig. 1 Craya-Herring basis vectors for the wavenumbers in an interacting wavenumber triad $(\mathbf{k}', \mathbf{p}, \mathbf{q})$. From Verma [35]. Reprinted with permission from Verma.

$$d\hat{p} = \frac{1}{(2\pi)^{d+1}} d\mathbf{p} d\omega_p. \quad (13)$$

Field-theoretic computations are quite complex. However, Craya-Herring (CH) basis [12, 36, 37] simplifies these computations considerably [32, 38]. In 3D, the CH basis vectors are:

$$\hat{e}_0(\mathbf{k}) = \hat{k}; \quad \hat{e}_1(\mathbf{k}) = \frac{\hat{k} \times \hat{n}}{|\hat{k} \times \hat{n}|}; \quad \hat{e}_2(\mathbf{k}) = \hat{e}_0(\mathbf{k}) \times \hat{e}_1(\mathbf{k}), \quad (14)$$

where the unit vector \hat{k} is along the wavenumber \mathbf{k} , and the unit vector \hat{n} is chosen along any direction. An incompressible flow has components $u_1(\mathbf{k})$ and $u_2(\mathbf{k})$ along the unit vectors $\hat{e}_1(\mathbf{k})$ and $\hat{e}_2(\mathbf{k})$, respectively. We consider an interacting wavenumber triad $(\mathbf{k}', \mathbf{p}, \mathbf{q})$ with $\mathbf{k}' + \mathbf{p} + \mathbf{q} = 0$, and $\mathbf{k}' = -\mathbf{k}$. We choose $\hat{n} = (\mathbf{q} \times \mathbf{p})/|\mathbf{q} \times \mathbf{p}|$ [12, 35, 39]. The Craya-Herring basis vectors for the interacting wavenumbers are illustrated in Fig. 1. Note that α, β, γ are the angles in front of k, p, q respectively. Verma [35] derived the following equations for the Craya-Herring components u_1 and u_2 shown in Fig. 1:

$$(\partial_t + \nu k^2)u_1(\mathbf{k}', t) = ik' \sin(\beta - \gamma)u_1^*(\mathbf{p}, t)u_1^*(\mathbf{q}, t) + f_1(\mathbf{k}', t), \quad (15)$$

$$(\partial_t + \nu k^2)u_1(\mathbf{p}, t) = ip \sin(\gamma - \alpha)u_1^*(\mathbf{q}, t)u_1^*(\mathbf{k}', t) + f_1(\mathbf{p}, t), \quad (16)$$

$$(\partial_t + \nu k^2)u_1(\mathbf{q}, t) = iq \sin(\alpha - \beta)u_1^*(\mathbf{p}, t)u_1^*(\mathbf{k}', t) + f_1(\mathbf{q}, t), \quad (17)$$

$$(\partial_t + \nu k^2)u_2(\mathbf{k}', t) = ik' \{\sin \gamma u_1^*(\mathbf{p}, t)u_2^*(\mathbf{q}, t) - \sin \beta u_1^*(\mathbf{q}, t)u_2^*(\mathbf{p}, t)\} + f_2(\mathbf{k}', t),$$

(18)

$$(\partial_t + \nu k^2)u_2(\mathbf{p}, t) = ip\{\sin \alpha u_1^*(\mathbf{q}, t)u_2^*(\mathbf{k}', t) - \sin \gamma u_1^*(\mathbf{k}', t)u_2^*(\mathbf{q}, t)\} + f_2(\mathbf{p}, t),$$

(19)

$$(\partial_t + \nu k^2)u_2(\mathbf{q}, t) = iq\{\sin \beta u_1^*(\mathbf{k}', t)u_2^*(\mathbf{p}, t) - \sin \alpha u_1^*(\mathbf{p}, t)u_2^*(\mathbf{k}', t)\} + f_2(\mathbf{q}, t),$$

(20)

where f_1 and f_2 are force components along \hat{e}_1 and \hat{e}_2 respectively. We need to integrate over all possible triads for the evolution of $\mathbf{u}(\mathbf{k}, t)$.

For hydrodynamic turbulence, the *modal energy* for wavenumber \mathbf{k} is

$$E(\mathbf{k}) = \frac{1}{2}|\mathbf{u}(\mathbf{k})|^2 = \begin{cases} \frac{1}{2}|u_1(\mathbf{k})|^2 & \text{for 2D} \\ \frac{1}{2}|u_1(\mathbf{k})|^2 + \frac{1}{2}|u_2(\mathbf{k})|^2 & \text{for 3D.} \end{cases} \quad (21)$$

For an isotropic flow, the spectral correlation $\langle |u_i(\mathbf{k})|^2 \rangle$ for the CH components $u_i(\mathbf{k})$ are equal¹. That is,

$$\langle |u_i(\mathbf{k})|^2 \rangle \equiv C(\mathbf{k}) = C(k) \quad (22)$$

for all i 's. That is, $\langle |u_i(\mathbf{k})|^2 \rangle$ depends only on the magnitude of \mathbf{k} , which is denoted by k . The total kinetic energy of the flow is

$$\frac{\langle u^2 \rangle}{2} = \int E(k)dk = \frac{1}{2} \int \frac{d\mathbf{k}}{(2\pi)^d} (d-1)C(\mathbf{k}) = \frac{1}{2} \frac{S_d}{(2\pi)^d} (d-1) \int dk k^{d-1} C(\mathbf{k}), \quad (23)$$

where $E(k)$ is the one-dimensional (1D) shell spectrum, and $S_d = 2\pi^{d/2}/\Gamma(d/2)$ is the surface area of the d -dimensional sphere. The above equation yields the following relationship between the modal energy and 1D energy spectrum [9, 21, 40]:

$$E(k) = \frac{(d-1)}{2} \frac{S_d k^{d-1}}{(2\pi)^d} C(\mathbf{k}). \quad (24)$$

In Kolmogorov's theory of turbulence [6, 7], 1D energy spectrum is

$$E(k) = K_{\text{Ko}} \Pi^{2/3} k^{-5/3}, \quad (25)$$

where K_{Ko} is Kolmogorov's constant, and Π is the inertial-range kinetic energy flux or the kinetic energy dissipation rate. Note, however, that the thermalized Euler turbulence (with $\nu = 0$) admits equilibrium solution, for which

$$E(k) \sim k^{d-1}. \quad (26)$$

This equilibrium solution has zero energy flux [5, 41].

In Section 3, I present how Kraichnan [21] computed the Green's function and renormalized viscosity using Direct Interaction Approximation (DIA).

¹In this paper, we denote $|u_1(\mathbf{k})|^2 = C_1(\mathbf{k})$ and $|u_2(\mathbf{k})|^2 = C_2(\mathbf{k})$.

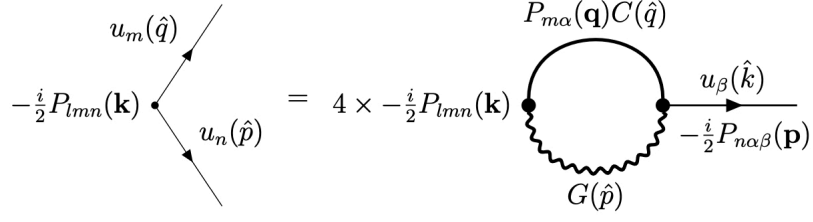


Fig. 2 Feynman diagrams associated with the computation of effective viscosity and Green's function using direct interaction approximation (DIA).

3 Direct Interaction Approximation (DIA)

The presentation in this section is a minor modification of Kraichnan [21]'s original calculation. Kraichnan [21] started with Eq. (9), and $\lambda = 1$ due to Galilean invariance. The *bare Green's function* for the linearized NS equation is

$$G(\hat{k}) = \frac{1}{-i\omega + \nu k^2}. \quad (27)$$

Kraichnan [21] treated the nonlinear term of the NS equation as perturbation. In addition, the velocity field is assumed to be homogeneous and quasi-Gaussian, which leads to

$$\langle u_m(\hat{q})u_n(\hat{p}) \rangle = C(\hat{q})P_{mn}(\mathbf{q})\delta(\mathbf{p} + \mathbf{q})\delta(\omega_p + \omega_q), \quad (28)$$

where $\hat{p} = (\omega_p, \mathbf{p})$ and $\hat{q} = (\omega_q, \mathbf{q})$. Under quasi-Gaussian approximation, the third-order correlation $\langle u_m(\hat{q})u_n(\hat{p})u_s(\hat{p}) \rangle$ is nonzero, and it is computed by expanding the velocity field perturbatively, and then reducing the fourth-order correlations to a sum of products of two second-order correlations.

To zeroth order, the ensemble-averaged value of the nonlinear term of Eq. (9) vanishes, i.e.,

$$P_{lmn}(\mathbf{k}) \langle u_m(\hat{q})u_n(\hat{p}) \rangle = 0 \quad (29)$$

because of Eq. (28) and $P_{lmn}(\mathbf{k} = 0) = 0$ [9, 21, 27]. Hence, Kraichnan [21] went to the next order, which is represented using the Feynman diagram of Fig. 2. To the first order, the transformed equation for the velocity field is [21]

$$(-i\omega + \nu k^2) u_l(\hat{k}) = -u_\beta(\hat{k}) \int d\hat{q} [G(\hat{p})C(\hat{q})A_{l\beta}(\mathbf{k}, \mathbf{p}, \mathbf{q})] + f_l(\hat{k}), \quad (30)$$

where

$$A_{l\beta}(\mathbf{k}, \mathbf{p}, \mathbf{q}) = P_{lmn}(\mathbf{k})P_{n\alpha\beta}(\mathbf{p})P_{m\alpha}(\mathbf{q}) \quad (31)$$

with the *effective* or *dressed Green's function* as

$$G(\hat{k}) = \frac{1}{-i\omega + \nu(k)k^2}, \quad (32)$$

and *dressed correlation function* as

$$\langle u_i^*(\hat{k})u_j(\hat{k}) \rangle = \frac{1}{-i\omega + \nu(k)k^2} C(\mathbf{k})P_{ij}(\mathbf{k}). \quad (33)$$

In terms of time variable,

$$G(\mathbf{k}, t - t') = H(t - t') \exp[-\nu(k)k^2(t - t')], \quad (34)$$

$$\bar{C}(\mathbf{k}, t - t') = C(\mathbf{k}) \exp[-\nu(k)k^2(t - t')], \quad (35)$$

where $H(t - t')$ is the heaviside function, which is 0 for $t < t'$ and 1 for $t > t'$. The above equations show that the two-time Green's function and correlations function decay with a time scale of $(\nu(k)k^2)^{-1}$, where $\nu(k)$ is the effective or dressed viscosity. This important assumption, employed in almost all turbulence calculations [8, 9, 21], is an extrapolation of *fluctuation-dissipation theorem* to systems far from equilibrium (see Section 10).

The nonlinear term of Eq. (30) is proportional to the velocity field. However, the velocity components in the left-hand side and right-hand side of Eq. (30) are unequal (u_l and u_β , respectively). Therefore, the viscosity correction due to the nonlinear term is a second-rank tensor:

$$\nu_{l\beta}(\mathbf{k}) = \int d\hat{q} G(\hat{p}) C(\hat{q}) A_{l\beta}(\mathbf{k}, \mathbf{p}, \mathbf{q}). \quad (36)$$

This feature appear surprising for an isotropic flow, but this is reasonable because the renormalized parameter in the plane of the triad $(\mathbf{k}, \mathbf{p}, \mathbf{q})$ may differ from that perpendicular to this plane². However, Kraichnan [21] and many other researchers have assumed the *dressed viscosity* to be an isotropic tensor, i.e.,

$$\nu_{l\beta}(\hat{k}) = \nu(\hat{k})P_{l\beta}(\mathbf{k}), \quad (37)$$

with

$$\nu(\hat{k}) = \frac{1}{(d-1)k^2} \int d\hat{p} Q(k, p, q) G(\hat{p}) C(\hat{q}), \quad (38)$$

where

$$Q(k, p, q) = P_{lmn}(\mathbf{k})P_{n\alpha\beta}(\mathbf{p})P_{m\alpha}(\mathbf{q})P_{l\beta}(\mathbf{k}) = pk[(d-3)z + 2z^3 + (d-1)xy]. \quad (39)$$

²Recently, Verma [32] observed such behaviour in his calculations based on Craya-Herring basis. See Section 4.3.

Using Eqs. (30, 37, 38), Eq. (9) is rewritten in terms of dressed viscosity as

$$(-i\omega + \nu k^2 + \nu(k)k^2) u_l(\hat{k}) = f_l(\hat{k}) \quad (40)$$

with

$$\nu(k) = \frac{1}{(d-1)k^2} \int \frac{d\mathbf{q}}{(2\pi)^d} \frac{Q(k, p, q)C(q)}{\nu(p)p^2 + \nu(q)q^2} \quad (41)$$

under the long time limit ($\omega \rightarrow 0$) [9, 13, 21, 42]. Kraichnan [21] attempted the self-consistent solution to Eq. (41) using $C(k)$ of Eq. (24, 25) and the following formula for $\nu(k)$ (based on Kolmogorov's spectrum):

$$\nu(k) = \nu_* \sqrt{K_{\text{Ko}}} \Pi_u^{2/3} k^{-4/3}, \quad (42)$$

where ν_* is a nondimensional constant. Further, he nondimensionalized Eq. (41) using $p = kp'$ and $q = kq'$ that yields

$$\nu_*^2 = \frac{2S_{d-1}}{S_d(d-1)^2} \int_0^\infty dq' q'^{d-1} \int_{-1}^1 dy (1-y^2)^{(d-3)/2} \frac{Q(1, p', q') q'^{-2/3-d}}{p'^{2/3} + q'^{2/3}}, \quad (43)$$

where $y = \cos \beta$ with β being the angle between \mathbf{k} and \mathbf{q} (see Fig. 1).

Unfortunately, the integral of Eq. (43) has infrared divergence near $p' = 0$. Kraichnan [21] tried to cure this divergence by introducing a lower or infrared cutoff for p' , but this trick leads to $k^{-3/2}$ energy spectrum that contradicts the popular Kolmogorov's theory. Leslie [9] attempted a k -dependent lower cutoff for p' , i.e., $p' \geq ck$ (c is a constant) that leads to Kolmogorov's spectrum. Inspired by the infinity cancellations employed in quantum electrodynamics [1], Leslie [9] suggested splitting the integral of Eq. (43) into singular and nonsingular parts; unfortunately, this idea has not been implemented till date.

Renormalization-Group (RG) is employed to solve the above divergence problem [1]. In Section 4, I describe viscosity renormalization based on Wilson's wavenumber RG scheme.

4 Renormalization Group Analysis of Hydrodynamic Turbulence

In this section, I will cover prominent HDT RG schemes, mainly that of Yakhot and Orszag (YO) [26], McComb [10], Zhou et al. [29], DeDominicis and Martin [30], and Verma et al. [43]. Following Wilson's wavenumber renormalization, the wavenumber space is logarithmic-binned with $k_m = k_0 c^m$ and $c > 1$. For the wavenumber up to k_{n+1} shown in Fig. 3, Eq. (9) is rewritten as

$$(-i\omega + \nu^{(n+1)}k^2) u_l^<(\hat{k}) = f_l(\hat{k}) - i \frac{\lambda}{2} P_{lmn}(\mathbf{k}) \int_{\hat{p}+\hat{q}=\hat{k}} d\hat{p} [u_m^<(\hat{q})u_n^<(\hat{p}) + u_m^>(\hat{q})u_n^>(\hat{p})]$$

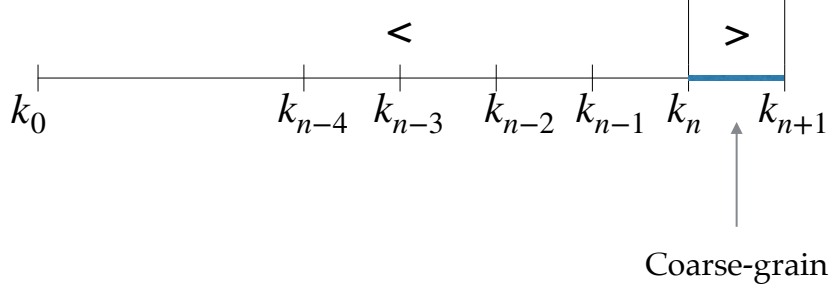


Fig. 3 In wavenumber renormalization, the modes in the wavenumber band (k_n, k_{n+1}) , denoted by $>$, are coarse-grained. The coarse-graining operation leads to enhancement of effective viscosity for wavenumbers $k < k_n$, denoted by $<$. From Verma [32]. Reprinted with permission from APS.

$$+ u_m^<(\hat{q})u_n^>(\hat{p}) + u_m^>(\hat{q})u_n^<(\hat{p})] \quad (44)$$

with $\hat{q} = \hat{k} - \hat{p}$. The convolutions in the above equation involves four sums with wavenumbers \mathbf{p} and \mathbf{q} belonging to $<$ or $>$ regions of Fig. 3. Now, we ensemble-average the fluctuations in wavenumber band (k_n, k_{n+1}) , after which $\nu_1^{(n)}$ is the viscosity for the wavenumbers (k_0, k_n) . The above averaging process is called *coarse graining*.

For the coarse-graining process, it is assumed that $u^>(\mathbf{k}, t)$ is time-stationary, homogeneous, isotropic, and Gaussian with zero mean, and that $u^<(\mathbf{k}, t)$ is unaffected by coarse-graining [4, 10, 16]. Another assumption is that the correlation between $<$ and $>$ modes is weak. Hence,

$$\langle u_i^>(\mathbf{k}, t) \rangle = 0, \quad (45)$$

$$\langle u_i^<(\mathbf{k}, t) \rangle = u_i^<(\mathbf{k}, t), \quad (46)$$

$$\langle u_i^{*<}(\mathbf{p}, t)u_m^{*<}(\mathbf{q}, t) \rangle = u_i^{*<}(\mathbf{p}, t)u_m^{*<}(\mathbf{q}, t), \quad (47)$$

$$\langle u_i^{*<}(\mathbf{p}, t)u_m^{*>}(\mathbf{q}, t) \rangle = u_i^{*<}(\mathbf{p}, t)\langle u_m^{*>}(\mathbf{q}, t) \rangle = 0, \quad (48)$$

$$\langle u_i^{*>}(\mathbf{p}, t)u_m^{*<}(\mathbf{q}, t) \rangle = \langle u_i^{*>}(\mathbf{p}, t) \rangle u_m^{*<}(\mathbf{q}, t) = 0. \quad (49)$$

Substitution of the above relations in Eq. (44) yields

$$\left(-i\omega + \nu^{(n)}k^2\right) u_i^<(\hat{k}) = f_i(\hat{k}) - i\frac{\lambda}{2}P_{lmn}(\mathbf{k}) \int_{\hat{p}+\hat{q}+\hat{k}} d\hat{p} [u_m^<(\hat{q})u_n^<(\hat{p})], \quad (50)$$

where

$$\nu^{(n)} = \nu^{(n+1)} + i \frac{\lambda}{2k^2} P_{lmn}(\mathbf{k}) \int^{\Delta} d\hat{p} \langle u_m^>(\hat{q}) u_n^>(\hat{p}) \rangle = \nu^{(n+1)} + \delta\nu^{(n)}, \quad (51)$$

with the integral performed over the coarse-grained region (Δ). This integral provides the viscosity correction ($\delta\nu^{(n)}$).

At this point, we pause our discussion on HDT and go to Euler turbulence. The velocity field of thermalized spectrally-truncated Euler equation is Gaussian. Hence, $\langle u_m^>(\hat{q}) u_n^>(\hat{p}) \rangle = 0$ leading to $\delta\nu^{(n)} = 0$. Thus, the viscosity of Euler equation remains unchanged at $\nu = 0$; this is the result of *equilibrium field theory*.

Under the quasi-Gaussian approximation, the integral of Eq. (51) vanishes to the zeroth order. Hence, the integral is expanded to the first-order. Researchers have adopted various tactics to compute $\delta\nu^{(n)}$. In the following subsections, we will describe the schemes adopted by Yakhot and Orszag [26], McComb and Shanmugasundaram [44], Zhou et al. [29], Verma [32], Martin et al. [31], and DeDominicis and Martin [30]. We start with Yakhot and Orszag [26]'s RG scheme.

4.1 RG Scheme of Yakhot and Orszag

Yakhot and Orszag [26] (YO) employed dynamical RG framework [45] that includes renormalization of viscosity, vertex, and forcing amplitude. In the NS equation, the vertex correction is absent due to the Galilean invariance. Therefore, Yakhot and Orszag [26] computed the corrections to viscosity and forcing amplitude.

Following statistical field theory, Yakhot and Orszag [26] employed the following random force:

$$\langle f_l(\mathbf{k}, \omega) f_m(\mathbf{k}', \omega') \rangle = 2Dk^{-y} P_{lm}(\mathbf{k}) \delta(\mathbf{k} + \mathbf{k}') \delta(\omega + \omega'). \quad (52)$$

Equation (3) provides the real space correlation for the above force (after the frequency integral). The velocity field in terms of Green's function is

$$u_l(\hat{k}) = G(\hat{k}) f_l(\hat{k}), \quad \text{or} \quad u_l(\mathbf{k}, \omega) = G(\mathbf{k}, \omega) f_l(\mathbf{k}, \omega). \quad (53)$$

Yakhot and Orszag [26] employed RG that includes (a) parameter corrections under coarse-graining, and then (b) system rescaling to get back to the original size. These steps are same as those in Wilson's framework [4]. We brief these two steps in the following discussion.

4.1.1 Coarse-graining

In Eq. (51), to zeroth order $\delta\nu^{(n)} = 0$ because of the same reasons given in Section 3 [refer to Eq. (29)]. Therefore, Yakhot and Orszag [26] computed the viscosity correction to the next order, which is represented by the Feynman diagram of Fig. 4. Here we assume *large time limit*, which is

$$\nu(k) = \lim_{\omega \rightarrow 0} \nu(k, \omega). \quad (54)$$

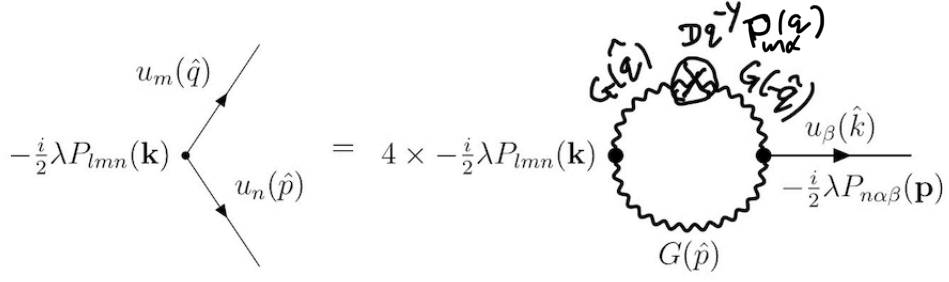


Fig. 4 Feynman diagrams associated with the computation of renormalized viscosity by Yakhot and Orszag [26].

Under these assumptions, the formula for the viscosity correction is

$$\begin{aligned}
\delta\nu(k) &= \lambda^2 \int \frac{d\mathbf{q}d\omega_q}{(2\pi)^{d+1}} Q(k, p, q) G(\hat{p}) G(\hat{q}) G(-\hat{q}) 2Dq^{-y} \\
&= \frac{\lambda^2}{2\nu^2} \int d\mathbf{q} Q(k, p, q) D \frac{q^{-y-2}}{p^2 + q^2} \\
&= \frac{\lambda^2}{2\nu^2} S_d \int_{\Lambda}^{\Lambda c} q^{d-1} dq \int_{-1}^1 dz (1-z^2)^{(d-3)/2} Q(k, p, q) D \frac{q^{-y-2}}{p^2 + q^2}, \\
&= \nu \bar{\lambda}^2 A_d \frac{e^{c\ell} - 1}{\epsilon},
\end{aligned} \tag{55}$$

where $c = e^\ell$, $z = \cos \gamma$ (see Fig. 1), $Q(k, p, q)$ are given in Eq. (39), and

$$\epsilon = 4 + y - d, \tag{56}$$

$$\bar{\lambda}^2 = \frac{\lambda^2 D}{\nu^3 \Lambda^\epsilon}, \tag{57}$$

$$A_d = \frac{1}{2} \frac{d^2 - d - \epsilon}{d(d+2)} \frac{S_d}{(2\pi)^d}. \tag{58}$$

Note that $\bar{\lambda}$ is the nondimensional coupling constant for HDT.

In Eq. (51), Yakhot and Orszag replaced $\nu^{(n+1)}$ with ν , and set $k_n \rightarrow \Lambda$ and $k_{n+1} \rightarrow \Lambda c$. Here, we have skipped some factors in Eq. (55), which have been absorbed in A_d . With $\delta\nu(k)$, the revised viscosity $\nu^< [\nu^{(n)}$ of Eq. (51)] is

$$\nu^< = \nu \left[1 + \bar{\lambda}^2 A_d \frac{e^{c\ell} - 1}{\epsilon} \right]. \tag{59}$$

The other two parameters to be renormalized are λ and D . Galilean invariance leads to constancy of λ , which is

$$\lambda^< = \lambda. \quad (60)$$

Yakhot and Orszag [26] argued that D too remains unrenormalized, or

$$D^< = D. \quad (61)$$

Equation (61) is consistent with Kolmogorov's theory of turbulence where forcing, applied at large scales, is absent in the inertial range. Hence, the forcing amplitude is not renormalized.

4.1.2 Rescaling

Under coarse-graining, the wavenumber range (k_0, k_{n+1}) shrinks to (k_0, k_n) (by a factor c^{-1}). Following Wilson [4], to rescale the system to its original size, we perform $k \rightarrow k' = kc$ that corresponds to $x = x'/c$. In all, we rescale x, t, u , and f as follows:

$$x = x'c; \quad t = t'c^z; \quad u = u'c^\chi; \quad f = c^{\frac{y-d-z}{2}} f', \quad (62)$$

where z and χ are constants that are determined using the RG analysis. Note that f scaling follows from Eq. (3). Therefore, under rescaling, the NS equation transforms to

$$\frac{\partial \mathbf{u}'}{\partial t'} - \nu^< c^{z-2} \nabla^2 \mathbf{u}' = -\lambda^< c^{\chi+z-1} [\mathbf{u}' \cdot \nabla' \mathbf{u}' - \nabla' p'] + c^{\frac{z+y-d}{2}-\chi} f'. \quad (63)$$

Hence, a combination of coarse-graining and rescaling yields [Eqs. (59, 60, 61, 63)]

$$\nu' = \nu^< c^{z-2}, \quad (64)$$

$$\lambda' = \lambda^< c^{\chi+z-1}, \quad (65)$$

$$D' = D^< c^{z+y-d-2\chi}. \quad (66)$$

Using $c = e^l$ and taking the limit $l \rightarrow 0$, we obtain

$$\frac{d\nu}{dl} = \nu [z - 2 + A_d \bar{\lambda}^2], \quad (67)$$

$$\frac{d\lambda}{dl} = \lambda [\chi + z - 1], \quad (68)$$

$$\frac{dD}{dl} = D [z + y - d - 2\chi]. \quad (69)$$

Equations (67, 68, 69) have a trivial fixed point, $(\nu = 0, \lambda = 0, D = 0)$, and the following nontrivial fixed point:

$$z = 2 - \frac{\epsilon}{3}, \quad (70)$$

$$\chi = \frac{\epsilon}{3} - 1, \quad (71)$$

where $\epsilon = 4 + y - d$ [see Eq. (56)]. We take derivative of $\bar{\lambda}$ [Eq. (57)] near the unstable fixed point [Eqs. (70, 71)] that yields

$$\frac{d\bar{\lambda}}{dl} = \frac{\bar{\lambda}}{2}(\epsilon - 3A_d\bar{\lambda}^2). \quad (72)$$

Hence, for $\epsilon < 0$, $\bar{\lambda} \rightarrow 0$ (trivial fixed point: $\nu = 0, \lambda = 0, D = 0$). Therefore, $\epsilon < 0$ leads to decoupled thermalized Fourier modes, similar to the Gaussian fixed point of ϕ^4 theory [1, 2, 4]. However, when $\epsilon > 0$, $\bar{\lambda}$ moves to

$$\bar{\lambda} = \sqrt{\frac{\epsilon}{3A_d}}, \quad (73)$$

thus making the nonlinear term relevant. The above calculation yields the RG fixed point for the nonequilibrium solution [Eqs. (70, 71, 73)], similar to ϕ^4 theory [1, 2, 4]. Note that $\bar{\lambda} = O(1)$ for the unstable fixed point.

Using this unstable RG fixed point, we derive the energy spectrum for HDT as follow. Using Eq. (62) we derive

$$\frac{u}{u'} = c^\chi = \left(\frac{k}{k'}\right)^{-\chi} \implies u_k \propto k^{-\chi}. \quad (74)$$

Hence,

$$E(k) \sim u_k^2/k \sim k^{-2\chi-1} \sim k^{-2\epsilon/3+1}. \quad (75)$$

We recover Kolmogorov's $k^{-5/3}$ spectrum when $\epsilon = 4$, or $y = d$. For this case, the forcing spectrum is k^{-d} , which is dominantly at large scales, as in Kolmogorov's theory of turbulence. Hence, YO's RG results are consistent with Kolmogorov's theory of turbulence.

In addition, for the Kolmogorov's spectrum,

$$z = 2 - \frac{\epsilon}{3} = \frac{2}{3} \implies \omega = k^z = k^{2/3}, \quad (76)$$

leading to the dynamic exponent to be $2/3$. Also, the renormalized viscosity (without rescaling) is

$$\nu^< = \nu(k) \sim \nu' b^{2-z} \sim k^{-4/3} \quad (77)$$

because ν' is a constant.

The external force injects energy to the mode $\mathbf{u}(\mathbf{k})$ with a rate of $\langle |\mathbf{f}(\mathbf{k})|^2 \rangle$. Here, we focus on the special case $y = d$ that yields $k^{-5/3}$ spectrum. The energy injection rate to the flow in a wavenumber shell (k_0, k) is [26]

$$\epsilon_{\text{inj}}(k) = 2D_0 \int_{k_0}^k k'^{-y} d\mathbf{k}'$$

$$\begin{aligned}
&= 2S_d D_0 \int_{k_0}^k k'^{-y+d-1} dk' \\
&= 2S_d D_0 \ln \frac{k}{k_0},
\end{aligned} \tag{78}$$

which is a slowly-varying logarithmic function of k , and it can be assumed to a constant.

According to the variable energy flux framework [46],

$$\frac{d\Pi(k)}{dk} = \mathcal{F}(k) - D(k) \tag{79}$$

where $\mathcal{F}(k)$ and $D(k)$ are, respectively, the energy injection rate and dissipation rate to the wavenumber shell of radius k . In YO formalism with $y = d$, we can assume that $\mathcal{F}(k) \rightarrow 0$ (due to steepness of $\mathcal{F}(k)$) and $D(k) \rightarrow 0$ in the inertial range. Hence, we obtain a nearly constant inertial-range energy flux:

$$\Pi(k) \approx \epsilon_{\text{inj}}. \tag{80}$$

Thus, YO formalism yields similar results as Kolmogorov's theory. Note, however, that in the inertial range, $\mathcal{F}(k) \sim 1/k$ in YO theory, but $\mathcal{F}(k) = 0$ in Kolmogorov theory.

In an earlier work, Forster et al. [27] employed a similar RG analysis for different forcing functions, and derived various $E(k)$'s, including $E(k) \sim k^2$ for 3D. We skip these derivations due to lack of space.

4.2 McComb and Zhou

McComb, Zhou, and coworkers [29, 44] performed self-consistent recursive RG analysis and computed the renormalized viscosity. They assumed the forcing to be at large scales, hence noise renormalization is not required in the inertial range, where power-law solution is attempted for the renormalized viscosity.

In the absence of noise, the Feynman diagrams for McComb and Zhou's RG procedure are same as that employed for DIA. McComb and Zhou performed only coarse-graining, and not rescaling, that leads to an increase in the renormalized viscosity increases to

$$\nu^{(n)}(k) = \nu^{(n+1)}(k) + \delta\nu^{(n)}(k). \tag{81}$$

For $\nu^{(n)}(k)$, McComb and Zhou employed power-law solution along with a universal function $\nu_{(n)}^*(k')$:

$$\nu^{(n)}(k_n k') = (K_{\text{Ko}})^{1/2} \Pi^{1/3} k_n^{-4/3} \nu_{(n)}^*(k'). \tag{82}$$

Substitution of Eqs. (81, 82) in Eq. (51) yields

$$\begin{aligned}
\delta\nu_{(n)}^*(k') &= \frac{1}{(d-1)} \int^{\Delta} d\mathbf{p}' \frac{2}{(d-1)S_d} \frac{E(q')}{q'^{d-1}} \left[\frac{Q(k', p', q')}{\nu_{(n)}^*(hp')p'^2 + \nu_{(n)}^*(hq')q'^2} \right], \\
\nu^{(n+1)*}(k') &= h^{4/3} \nu_{(n)}^*(hk') + h^{-4/3} \delta\nu_{(n)}^*(k'),
\end{aligned} \tag{83}$$

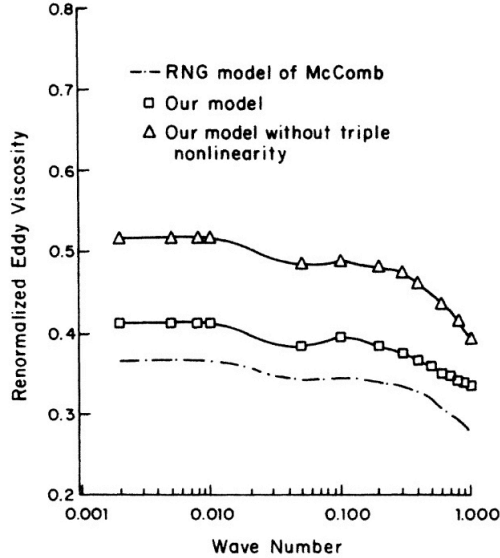


Fig. 5 Plot of $\nu_{(n)}^*(k')$ vs. k' computed by Zhou et al. [29] without $\langle u^<u^<u^<$ (solid line with squares) and with $\langle u^<u^<u^<$ (solid line with triangles), and by McComb (chained line). From Zhou et al. [29]. Reprinted with permission from APS.

where $Q(k', p', q')$ is given in Eq. (39), $\mathbf{p}' + \mathbf{q}' = \mathbf{k}'$, and $h = 1/c$ with $c = k_{n+1}/k_n$ as the coarse-graining parameter.

The $d\mathbf{p}'$ integral of Eq. (83) is computed in the wavenumber band $k_n \leq p < k_{n+1}$ and $k_n \leq q < k_{n+1}$. McComb, Zhou, and coworkers solved the above equations numerically that yields $\nu_{(n)}^*(k')$ shown in Fig. 5. Zhou et al. [29] reported that $\nu_{(n)}^*(k') \rightarrow 0.4$ for small k' , whereas McComb and Shanmugasundaram [44] reported that $\nu_{(n)}^*(k') \rightarrow 0.37$. Zhou et al. [29] argued that an inclusion of triple nonlinearity, $\langle u^<u^<u^<$, alters $\nu_{(n)}^*(k')$ marginally (see Fig. 5); but this issue is beyond the scope of this paper.

4.3 RG Analysis in Craya-Herring Basis

RG analysis is quite complex involving intricate tensor algebra and integrals. Recently, Verma [32] employed the Craya-Herring (CH) basis that simplifies the algebra significantly. In addition, similarities between hydrodynamic, scalar, and magnetohydrodynamic (MHD) turbulence become apparent in CH basis. We will discuss these similarities in Sections 6 and 7.

Verma [32] focussed on the triadic interactions in the CH basis. As shown in Fig. 1, for a triad, the u_1 components reside in the plane of the triad, whereas the u_2 components are perpendicular to the plane. Verma [32] showed that the renormalized viscosities of the u_1 and u_2 components are different, which has many important implications. For example, this feature leads to a conclusion that $d = 6$ is the critical upper dimension for HDT [32].

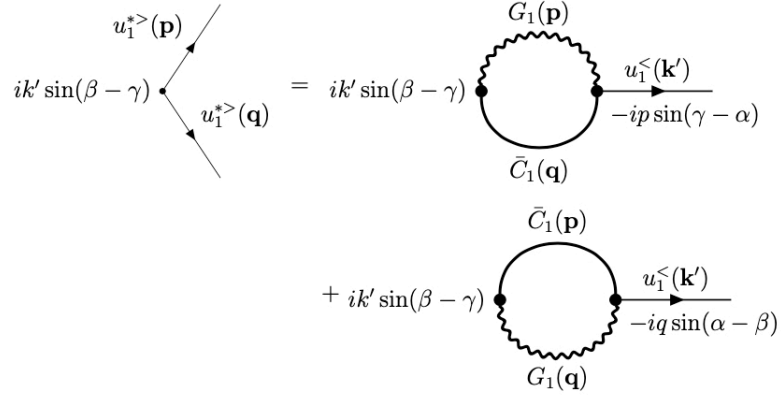


Fig. 6 Feynman diagrams associated with the renormalization of ν_1 for the u_1 component. From Verma [32]. Reprinted with permission from APS.

In this subsection, we briefly describe the renormalization of the viscosities ν_1 and ν_2 (for u_1 and u_2 , respectively) [32]. We start with Eqs. (15, 18) and compute the viscosity corrections arising due to the nonlinear terms. The Feynman diagrams for the ν_1 and ν_2 corrections are illustrated in Fig. 6 and Fig. 7, respectively. These computations lead to

$$\nu_1^{(n)} k^2 = \nu_1^{(n+1)} k^2 - \text{Integrals corresponding to Fig. 6}, \quad (85)$$

$$\nu_2^{(n)} k^2 = \nu_2^{(n+1)} k^2 - \text{Integrals corresponding to Fig. 7}, \quad (86)$$

or

$$\nu_1^{(n)} k^2 = \nu_1^{(n+1)} k^2 - \int_{\Delta} \frac{d\mathbf{p}}{(2\pi)^d} \frac{k \sin(\beta - \gamma)}{\nu_1(p)p^2 + \nu_1(q)q^2} [pC_1(\mathbf{q}) \sin(\gamma - \alpha) + qC_1(\mathbf{p}) \sin(\alpha - \beta)], \quad (87)$$

$$\nu_2^{(n)} k^2 = \nu_2^{(n+1)} k^2 - \int_{\Delta} \frac{d\mathbf{p}}{(2\pi)^d} \left[\frac{kqC_1(\mathbf{p}) \sin \gamma \sin \alpha}{\nu_1(p)p^2 + \nu_2(q)q^2} + \frac{kpC_1(\mathbf{q}) \sin \beta \sin \alpha}{\nu_2(p)p^2 + \nu_1(q)q^2} \right]. \quad (88)$$

Following Kolmogorov's theory of turbulence, we model $\nu_1^{(n)}$ and $\nu_2^{(n)}$ as follows:

$$\nu_1^{(n)} = \nu_{1*} \sqrt{K_{\text{Ko}}} \Pi^{1/3} k_n^{-4/3}, \quad (89)$$

$$\nu_2^{(n)} = \nu_{2*} \sqrt{K_{\text{Ko}}} \Pi^{1/3} k_n^{-4/3}. \quad (90)$$

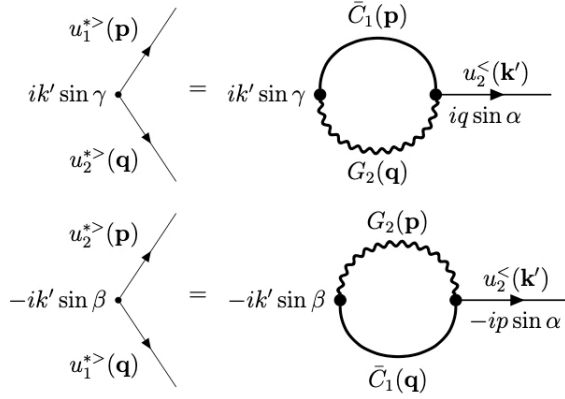


Fig. 7 Feynman diagrams associated with the renormalization of ν_2 for the u_2 component. Modified version of Fig. 7 of Verma [32]. Reprinted with permission from APS.

Substitution of Eqs. (89, 90) and Kolmogorov's energy spectrum [Eqs. (24, 25)] in Eqs. (87, 88) yields

$$\nu_{1*}(1 - b^{-4/3}) = -\frac{2S_{d-1}}{(d-1)S_d} \frac{1}{\nu_{1*}} \int_1^b p'^{d-1} dp' \int_{(p'^2+1-b^2)/(2p')}^{p'/2} dz (1-z^2)^{\frac{d-3}{2}} (F_1 + F_2), \quad (91)$$

$$\nu_{2*}(1 - b^{-4/3}) = \frac{2S_{d-1}}{(d-1)S_d} \int_1^b p'^{d-1} dp' \int_{(p'^2+1-b^2)/(2p')}^{p'/2} dz (1-z^2)^{\frac{d-3}{2}} F_3(p', z), \quad (92)$$

where

$$F_1(p', z) = \frac{(1-z^2)(p' - 2z)(2p'z - 1)p'q'^{-8/3-d}}{p'^{2/3} + q'^{2/3}}, \quad (93)$$

$$F_2(p', z) = \frac{(1-z^2)(1-p'^2)(2p'z - 1)p'^{-2/3-d}q'^{-2}}{p'^{2/3} + q'^{2/3}}, \quad (94)$$

$$F_3(p', z) = \frac{(1-z^2)p'^{-2/3-d}}{\nu_{1*}p'^{2/3} + \nu_{2*}q'^{2/3}} + \frac{(1-z^2)p'^2q'^{-8/3-d}}{\nu_{2*}p'^{2/3} + \nu_{1*}q'^{2/3}}. \quad (95)$$

See Verma [32] for details.

For $c = 1.5$, the integrals yield $\nu_{1*} = 0.098$ and $\nu_{2*} = 0.62$ for 2D HDT, and $\nu_{1*} = 0.070$ and $\nu_{2*} = 0.53$ for 3D HDT [32]. These constants are reasonably close to those reported by McComb [10] and Zhou et al. [29]. Verma [32] also showed that ν_{1*} vanishes for $d = 6$, which leads to the upper critical dimension for HDT to be 6. That is, the velocity field is Gaussian for $d \geq 6$ [32].

4.4 Functional RG

In statistical field theory, *partition function* is computed using functional integral of *order parameter*. Similarly, quantum field theory employs functional integrals for many computations. The above computations are mostly for equilibrium fields. Fortunately, functional integral has been applied to turbulence with some modifications in the standard framework [19, 30, 47].

DeDominicis and Martin [30] started with the following equations:

$$\partial_t u_\alpha = \nu_0 \nabla^2 u_\alpha + \lambda_0 \tau_{\alpha\beta} (\mathbf{u} \cdot \nabla) u_\beta + f_\alpha, \quad (96)$$

$$\tau_{\alpha\beta} = \delta_{\alpha\beta} - \frac{k_\alpha k_\beta}{k^2}, \quad (97)$$

for which the *generating functional* was proposed as

$$\hat{Z}(l) = \int Du D\hat{u} \exp(\mathcal{L}[u, \hat{u}]) + \int dt d^d x l_\alpha(x, t) u_\alpha(x, t) \quad (98)$$

with the Lagrangian as

$$\mathcal{L} = \int dt d^d x [-i\hat{u}_\alpha (\partial_t - \nu_0 \nabla^2) u_\alpha - i\hat{u}_\alpha \lambda_0 \tau_{\alpha\beta} (\mathbf{u} \cdot \nabla) u_\beta + i\hat{u}_\alpha \langle f_\alpha f_\beta \rangle \hat{u}_\beta]. \quad (99)$$

Here, \hat{u} is the auxiliary function to u . Refer to Antonov et al. [19] for details.

DeDominicis and Martin [30] showed that the unperturbed propagators are

$$\langle i\hat{u}_\alpha u_\beta \rangle = \frac{1}{-i\omega + \nu_0 k^2} \delta_{\alpha\beta}, \quad (100)$$

$$\langle u_\alpha u_\beta \rangle = \frac{2D_0 k^{4-d}}{|-i\omega + \nu_0 k^2|^2} (m_0^2 + k^2)^{-y/2} \tau_{\alpha\beta}(k). \quad (101)$$

After some algebra, the relationship between the correlation and Green's functions was derived as

$$\langle uu \rangle = C(k, \omega) = \frac{D_0}{\nu_0^2} G\left(\frac{\omega}{i\nu_0}, k; g_0, \Lambda, m_0\right) \quad (102)$$

with

$$\frac{\lambda_0^2 D_0}{\nu_0^3} = g_0 \Lambda^y. \quad (103)$$

Using Callan-Symanzik equation, DeDominicis and Martin [30] derived that

$$E(k) \sim k^{-y+1+\eta_\nu-\eta_D}. \quad (104)$$

DeDominicis and Martin [30] showed that for small y and $d > 2$, $\eta_D = 0$ and $\eta_\nu = y/3$. For $y = 4$, $E(k) \sim k^{-5/3}$.

We end this section with a summary of RG analysis of HDT. RG solves the infrared divergence problem encountered in DIA. In addition, RG predicts both the equilibrium solution (k^{d-1} spectrum) and nonequilibrium solution ($k^{-5/3}$ spectrum) for HDT.

Note that RG analysis yields the latter solution even though the coupling constant is $O(1)$. RG computations also show that $d_c = 6$ is the critical dimension for HDT; for $d > d_c$, the velocity field is Gaussian, as in ϕ^4 theory for $d > 4$ [2, 4].

In Section 5, I will describe field-theoretic calculations of the energy transfers and flux in HDT.

5 Energy Transfers and Flux

In this section, we compute the energy fluxes in HDT, both in 2D and 3D. Here, nonzero fluxes arise due to the nonequilibrium nature of the flow.

5.1 Basic Formulas

The dynamical equation for the *modal energy* $E(\mathbf{k}) = |\mathbf{u}(\mathbf{k})|^2/2$ is [9, 21]

$$(\partial_t + 2\nu k^2)E(\mathbf{k}, t) = \frac{1}{2} \sum_{\mathbf{p}, \mathbf{q}} S^{uu}(\mathbf{k}|\mathbf{p}, \mathbf{q}) + \Re[\mathbf{F}_u(\mathbf{k}, t) \cdot \mathbf{u}^*(\mathbf{k}, t)], \quad (105)$$

where

1. $\Re[\mathbf{F}_u(\mathbf{k}, t) \cdot \mathbf{u}^*(\mathbf{k}, t)]$ represents energy injection to the wavenumber \mathbf{k} .
2. $2\nu k^2 E(\mathbf{k}, t)$ represents the viscous dissipation rate for the mode $E(\mathbf{k}, t)$.
3. The term

$$S^{uu}(\mathbf{k}|\mathbf{p}, \mathbf{q}) = \Im \{ \{ \mathbf{k} \cdot \mathbf{u}(\mathbf{q}, t) \} \{ \mathbf{u}(\mathbf{p}, t) \cdot \mathbf{u}^*(\mathbf{k}, t) \} \} + \{ \mathbf{k} \cdot \mathbf{u}(\mathbf{p}, t) \} \{ \mathbf{u}(\mathbf{q}, t) \cdot \mathbf{u}^*(\mathbf{k}, t) \} \} \quad (106)$$

is the *combined energy transfer* from $\mathbf{u}(\mathbf{q})$ and $\mathbf{u}(\mathbf{p})$ to $\mathbf{u}(\mathbf{k})$ [21].

Now, let us consider a wavenumber sphere of radius R . The external force injects energy into the sphere at the rate of $\sum_{k < R} \Re[\mathbf{F}_u(\mathbf{k}, t) \cdot \mathbf{u}^*(\mathbf{k}, t)]$. In Kolmogorov's theory of turbulence, the energy is injected at large scales *only*. In 3D, nonlinearity helps transfer this energy to small scales where it is dissipated by the viscous term. An absence of forcing in the inertial range leads to a constant energy flux in the inertial range [20, 46] [see Eq. (79)]. This phenomenology has some similarities with Yakhot-Orszag [26]'s RG predictions when $\epsilon = 4$. For this case, Yakhot and Orszag [26] obtained nearly constant energy flux and $k^{-5/3}$ energy spectrum in the inertial range (see Section 4.1).

The energy flux $\Pi(R)$ for the wavenumber sphere of radius R is the net nonlinear energy transfer rate from all the modes residing inside the sphere to the modes outside the sphere. Using $S(\mathbf{k}|\mathbf{p}, \mathbf{q})$, Kraichnan [21] derived the following formula for $\Pi(R)$ [9]:

$$\Pi(R) = \frac{1}{2} \int_R^\infty dk' \int \int^\Delta dpdq S(\mathbf{k}'|\mathbf{p}, \mathbf{q}) - \frac{1}{2} \int_0^R dk' \int \int^\Delta dpdq S(\mathbf{k}'|\mathbf{p}, \mathbf{q}), \quad (107)$$

where $\mathbf{k} = \mathbf{p} + \mathbf{q}$, and Δ represents a range of \mathbf{p}, \mathbf{q} consistent with the definition of energy flux [9, 21].

Dar et al. [48] and Verma [35, 40] showed that

$$S^{uu}(\mathbf{k}|\mathbf{p}|\mathbf{q}) = \Im \{ \{ \mathbf{k} \cdot \mathbf{u}(\mathbf{q}, t) \} \{ \mathbf{u}(\mathbf{p}, t) \cdot \mathbf{u}^*(\mathbf{k}, t) \} \} \quad (108)$$

is the *mode-to-mode energy transfer rate* from the *giver* mode $\mathbf{u}(\mathbf{p})$ to the *receiver* mode $\mathbf{u}(\mathbf{k})$ with the mediation of mode $\mathbf{u}(\mathbf{q})$. The combined energy transfer to \mathbf{k} from \mathbf{p} and \mathbf{q} is a sum of $S^{uu}(\mathbf{k}|\mathbf{p}|\mathbf{q})$ and $S^{uu}(\mathbf{k}|\mathbf{q}|\mathbf{p})$. In terms of $S^{uu}(\mathbf{k}|\mathbf{p}|\mathbf{q})$, the formula for $\Pi(R)$ is

$$\Pi(R) = \int_R^\infty \frac{d\mathbf{k}'}{(2\pi)^d} \int_0^R \frac{d\mathbf{p}}{(2\pi)^d} S^{uu}(\mathbf{k}'|\mathbf{p}|\mathbf{q}). \quad (109)$$

In Eq. (109), the giver modes are within the sphere, whereas the receiver modes are outside the sphere. In contrast, Kraichnan [21]'s derivation of Eq. (107) is longer and more complex. Note that Eqs. (107, 109) yield the same energy flux for a given velocity field [35, 40].

In Craya-Herring basis [32, 35],

$$S^{uu}(\mathbf{k}'|\mathbf{p}|\mathbf{q}) = S^{u_1 u_1}(\mathbf{k}'|\mathbf{p}|\mathbf{q}) + S^{u_2 u_2}(\mathbf{k}'|\mathbf{p}|\mathbf{q}), \quad (110)$$

where

$$S^{u_1 u_1}(\mathbf{k}'|\mathbf{p}|\mathbf{q}) = k' \sin \beta \cos \gamma \Im \{ u_1(\mathbf{q}, t) u_1(\mathbf{p}, t) u_1(\mathbf{k}', t) \}, \quad (111)$$

$$S^{u_2 u_2}(\mathbf{k}'|\mathbf{p}|\mathbf{q}) = -k' \sin \beta \Im \{ u_1(\mathbf{q}, t) u_2(\mathbf{p}, t) u_2(\mathbf{k}', t) \}. \quad (112)$$

Thus, there are independent energy transfers along the u_1 and u_2 channels, with no cross transfers between them.

5.2 Field-theoretic Computation of Energy Flux

Experiments and numerical simulations reveal that $\langle S^{uu}(\mathbf{k}'|\mathbf{p}|\mathbf{q}) \rangle \neq 0$ for HDT. Nonvanishing $S^{uu}(\mathbf{k}'|\mathbf{p}|\mathbf{q})$ (a triple correlation) indicates non-Gaussian and nonequilibrium nature of a turbulent flow. Interestingly, quasi-normal approximation for the triple correlation yields constant energy flux in the inertial range of HDT [9, 13, 21]. I briefly present this derivation in this subsection.

Under the quasi-normal approximation, the triple correlation of $S^{uu}(\mathbf{k}'|\mathbf{p}|\mathbf{q})$ vanishes to the zeroth order. However, the first-order expansion of the triple correlation yields a sum of fourth-order correlations, which are expanded as respective sums of products of two second-order correlations (assuming Gaussian distribution). Kolmogorov's energy spectrum and the renormalized viscosity are employed to compute the flux integrals.

Kraichnan [21] (also see Leslie [9]) was first to compute the turbulence flux using the above framework. By expanding Eq. (107) to first order, Kraichnan derived the following formula for 3D HDT:

$$1 = \frac{\langle \Pi(R) \rangle}{\Pi} = \frac{1}{K_{\text{Ko}}^{3/2}} \int_0^1 dv [\ln(1/v)] \int_{v^*}^{1+v} dv \Sigma(v, w), \quad (113)$$

where $v_* = \max(v, |1 - v|)$, and

$$\Sigma(v, w) = vw \frac{\{b(1, v, w)w^{-11/3}(v^{-11/3} - 1) + b(1, w, v)v^{-11/3}(w^{-11/3} - 1)\}}{1 + v^{2/3} + w^{2/3}} \quad (114)$$

with

$$b(1, v, w) = \frac{p}{k}(xy + z^3) \quad (115)$$

for 3D. The above derivation employs the following transformation [9, 21]

$$k = \frac{R}{u}; \quad p = \frac{Rv}{u}; \quad q = \frac{Rw}{u}. \quad (116)$$

Kraichnan [21] and Leslie [9] computed the integral of Eq. (113) numerically and reported the Kolmogorov's constant for 3D HDT to be near 1.6. Refer to Leslie [9] for details. Verma [40, 42] performed similar computations using the mode-to-mode energy transfers [40].

In the following discussion, we present the energy flux computations in the Craya-Herring basis [32]. Starting from Eq. (111), Verma [32] derived the following equation for the u_1 component:

$$\langle S^{u_1 u_1}(\mathbf{k}'|\mathbf{p}|\mathbf{q}) \rangle = \frac{\text{numr}_1}{\nu_1(k)k^2 + \nu_1(p)p^2 + \nu_1(q)q^2}, \quad (117)$$

where

$$\begin{aligned} \text{numr}_1 = & 2[k' \sin(\beta - \gamma)C_1(\mathbf{p})C_1(\mathbf{q}) + p \sin(\gamma - \alpha)C_1(\mathbf{k}')C_1(\mathbf{q}) + q \sin(\alpha - \beta)C_1(\mathbf{k}')C_1(\mathbf{p})] \\ & \times k' \sin \beta \cos \gamma. \end{aligned} \quad (118)$$

The three terms of $\langle S^{u_1 u_1}(\mathbf{k}'|\mathbf{p}|\mathbf{q}) \rangle$ correspond to the three Feynman diagrams of Fig. 8. For 3D and two-dimension three-component (2D3C), the energy transfers along the u_2 channel is

$$\langle S^{u_2 u_2}(\mathbf{k}'|\mathbf{p}|\mathbf{q}) \rangle = (k \sin \beta)^2 \frac{C_1(\mathbf{q})[C_2(\mathbf{p}) - C_2(\mathbf{k}')] }{\nu_2(k)k^2 + \nu_2(p)p^2 + \nu_1(q)q^2}. \quad (119)$$

The corresponding Feynman diagrams are shown in Fig. 9.

Using Eqs. (117, 119), we derive the corresponding energy fluxes:

$$\langle \Pi_{u_j}(R) \rangle = \int_R^\infty \frac{d\mathbf{k}'}{(2\pi)^d} \int_0^R \frac{d\mathbf{p}}{(2\pi)^d} \langle S^{u_j u_j}(\mathbf{k}'|\mathbf{p}|\mathbf{q}) \rangle, \quad (120)$$

where j takes values 1 or 2. Using the transformations of Eq. (116), Verma [32] derived the following nondimensionalized equation for $\langle \Pi_{u_j}(R) \rangle$:

$$\frac{\langle \Pi_{u_j}(R) \rangle}{\Pi} = A \int_0^1 dv [\log(1/v)] v^{d-1} \int_{-1}^1 dz (1 - z^2)^{\frac{d-3}{2}} \langle S^{u_j u_j}(v, z) \rangle, \quad (121)$$

$$\begin{aligned}
& \begin{array}{c} u_1(\mathbf{k}') \\ \nearrow \\ k' \sin \beta \cos \gamma \leftarrow u_1(\mathbf{p}) \\ \leftarrow \\ u_1(\mathbf{q}) \searrow \end{array} = 2 \times k' \sin \beta \cos \gamma \begin{array}{c} G_1(\mathbf{k}') \\ \text{---} \text{---} \text{---} \\ \bar{C}_1(\mathbf{p}) \\ \text{---} \text{---} \text{---} \\ \bar{C}_1(\mathbf{q}) \end{array} ik' \sin(\beta - \gamma) \\
& + 2 \times k' \sin \beta \cos \gamma \begin{array}{c} \bar{C}_1(\mathbf{k}') \\ \text{---} \text{---} \text{---} \\ G_1(\mathbf{p}) \\ \text{---} \text{---} \text{---} \\ \bar{C}_1(\mathbf{q}) \end{array} ip \sin(\gamma - \alpha) \\
& + 2 \times k' \sin \beta \cos \gamma \begin{array}{c} \bar{C}_1(\mathbf{k}') \\ \text{---} \text{---} \text{---} \\ \bar{C}_1(\mathbf{p}) \\ \text{---} \text{---} \text{---} \\ G_1(\mathbf{q}) \end{array} iq \sin(\alpha - \beta)
\end{aligned}$$

Fig. 8 Feynman diagrams associated with the energy transfers between the u_1 components. From Verma [32]. Reprinted with permission from APS.

$$\begin{aligned}
& \begin{array}{c} u_2(\mathbf{k}') \\ \nearrow \\ -k' \sin \beta \leftarrow u_2(\mathbf{p}) \\ \leftarrow \\ u_1(\mathbf{q}) \searrow \end{array} = -k' \sin \beta \begin{array}{c} G_2(\mathbf{k}') \\ \text{---} \text{---} \text{---} \\ \bar{C}_2(\mathbf{p}) \\ \text{---} \text{---} \text{---} \\ \bar{C}_1(\mathbf{q}) \end{array} -ik' \sin \beta \\
& + -k' \sin \beta \begin{array}{c} \bar{C}_2(\mathbf{k}') \\ \text{---} \text{---} \text{---} \\ G_2(\mathbf{p}) \\ \text{---} \text{---} \text{---} \\ \bar{C}_1(\mathbf{q}) \end{array} ip \sin \alpha
\end{aligned}$$

Fig. 9 Feynman diagrams associated with the energy transfers between the u_2 components. Modified version of Fig. 9 of Verma [32]. Reprinted with permission from APS.

where

$$A = K_{\text{Ko}}^{3/2} \frac{4}{(d-1)^2} \frac{S_{d-1}}{S_d}. \quad (122)$$

For 2D, the energy flux is $\Pi_{u_1}(R)$, whereas in 2D and 2D3C, the total energy flux is

$$\Pi(R) = \Pi_{u_1}(R) + \Pi_{u_2}(R). \quad (123)$$

See Verma [32] for details.

Verma [32] computed the energy fluxes for 2D and 3D turbulence. For 2D, using $\Pi_{u_1}(R) = -\Pi$ and $\nu_{1*} = 0.098$, Verma deduced that $K_{\text{Ko}} = 1.19$, which is inconsistent with numerical simulations and experiments, according to which $K_{\text{Ko}} \approx 6$, and with field-theoretic work of Nandy and Bhattacharjee [49], who reported that $K_{\text{Ko}} = 6.447$. These differences are possibly due to the inability of the recursive RG schemes to capture the nonlocal interactions. Verma [32] proposed a workaround by changing $\int_0^1 dv$ of Eq. (121) to $\int_{0.22}^1 dv$ that yields $K_{\text{Ko}} = 4.46$.

For 3D HDT, ν_{1*} and ν_{2*} appear in the denominator of Eq. (117, 119). Since $\nu_{1*} \ll \nu_{2*}$, the negative energy flux Π_{u_1} dominates positive Π_{u_2} leading to $\Pi(R) < 0$, which is inconsistent with the experimental and numerical observations. Fortunately, this issue is easily resolved by employing $\int_{0.22}^1 dv$ for $\Pi_{u_1}(R)$ of Eq. (121) that yields $K_{\text{Ko}} = 1.63$, which is in good agreement with earlier field-theoretic computations, as well as numerical and experimental results [32].

The above nonzero energy flux (nonequilibrium) breaks detailed balance via directional energy transfers—from small wavenumber modes to large wavenumbers. In contrast, the equilibrium solution, Gaussian velocity field of the spectrally-truncated Euler equation, respects detailed balance and yields vanishing energy flux. Note that the triple correlations of Eqs. (108, 117, 119) vanish following the Gaussian \mathbf{u} of the Euler turbulence [32, 35]. This is consistent with the fact that $\langle S^{u_j u_j}(\mathbf{k}'|\mathbf{p}|\mathbf{q}) \rangle$'s of Eqs. (117, 119) vanish for equipartitioned $C_1(\mathbf{k})$ and $C_2(\mathbf{k})$. Thus, field theory yields the energy transfers for the equilibrium flows (Euler turbulence) and nonequilibrium flows (HDT).

We end this section with a brief-comment on d -dimensional turbulence. Fournier and Frisch [50] employed eddy-damped quasi-normal Markovian (EDQNM) procedure to HDT and observed a transition from a positive energy flux to a negative energy flux near $d = 2.05$ as d decreases from 3 to 2. Adzhemyan et al. [51] employed perturbative field theory and showed that the Kolmogorov constant $K_{\text{Ko}} \propto d^{1/3}$, which leads to a decrease in the energy flux with the increase in d . Clark et al. [52] observed a transition to a non-chaotic regime above critical dimension $d_c \approx 5.88$. Recently, Verma [32] showed that $\nu_{1*} \rightarrow 0$ as $d \rightarrow 6$, and identified $d_c = 6$ as the critical dimension of HDT. The works by Clark et al. [52] and Verma [32] indicate that the velocity field becomes Gaussian for $d \approx 6$ and beyond. Field-theoretic work of Adzhemyan et al. [51] is consistent with the above conclusion.

Many realistic flows are accompanied by scalars (e.g., pollutants, temperature field) or vectors (e.g., magnetic field) or tensors (e.g., polymers). Field-theoretic treatment of such fields have yielded interesting results (see e.g., [16, 40, 53]). This topic is extensive

and its complete overview is beyond the scope of this review (see [9, 10, 12, 16, 17] for discussion). Yet, for illustration, we briefly describe two cases: a passive scalar advected by the velocity field, and a specific case of magnetohydrodynamic (MHD) turbulence.

6 Field-theoretic Treatment of Passive Scalar

In this section, I discuss a field-theoretic calculation of passive scalar turbulence. In this system, the momentum equation is not coupled to the scalar field. Hence, the equation for the velocity field is same as Eq. (1). The scalar field ψ is advected by the velocity field, hence its equation is [8, 9]

$$\frac{\partial \psi}{\partial t} + (\mathbf{u} \cdot \nabla) \psi = \kappa \nabla^2 \psi + f_\psi, \quad (124)$$

where f_ψ is the large-scale force on ψ , and κ is the scalar diffusion coefficient.

Equation (124) is transformed to Fourier space. In the CH basis, the evolution equation for $\psi(\mathbf{k}')$ is [35]

$$\left(\frac{\partial}{\partial t} + \kappa k^2 \right) \psi(\mathbf{k}') = ik' \int \frac{d\mathbf{p}}{(2\pi)^d} \{ \sin \gamma u_1^*(\mathbf{p}) \psi^*(\mathbf{q}) - \sin \beta u_1^*(\mathbf{q}) \psi^*(\mathbf{p}) \} + f_\psi(\mathbf{k}'), \quad (125)$$

where $\mathbf{k}' + \mathbf{p} + \mathbf{q} = 0$. Since Eq. (125) is same as that for $u_2(\mathbf{k})$ with $u_2 \rightarrow \psi$, we expect the RG and the energy-transfer equations for the scalar field to be similar to that for u_2 . This observation provides very useful insights.

For the scalar field, the correlation function at wavenumber \mathbf{k} is

$$C^\psi(\mathbf{k}) = |\psi(\mathbf{k})|^2, \quad (126)$$

and the total scalar energy is

$$\frac{\langle \psi^2 \rangle}{2} = \int E^\psi(k) dk = \frac{1}{2} \int \frac{d\mathbf{k}}{(2\pi)^d} C^\psi(\mathbf{k}) = \frac{1}{2} \frac{S_d}{(2\pi)^d} \int dk k^{d-1} C^\psi(\mathbf{k}), \quad (127)$$

where $E^\psi(k)$ is the one-dimensional (1D) shell spectrum. Using the above equation we derive

$$E^\psi(k) = \frac{1}{2} \frac{S_d k^{d-1}}{(2\pi)^d} C^\psi(\mathbf{k}). \quad (128)$$

The above $E^\psi(k)$ differs from 1D kinetic energy spectrum of Eq. (24) by a factor of $1/(d-1)$, which has important implications, as we show below.

For large Reynolds number $UL/\nu \gg 1$, the kinetic energy spectrum $E(k)$ is given by Eq. (25). For the turbulent velocity field, the passive scalar spectrum depends on the Péclet number, UL/κ , that represents the ratio of the nonlinear term $\mathbf{u} \cdot \nabla \psi$ and the diffusion term [54]. For large Reynolds and Péclet numbers, Oboukhov [55] and

Corrsin [56] proposed that the passive scalar spectrum is

$$E^\psi(k) = K_\psi \Pi_\psi \Pi^{-1/3} k^{-5/3}, \quad (129)$$

where Π_ψ is the *scalar energy flux*, and K_ψ is *Obukhov-Corrsin constant*. Using atmospheric boundary layer data, Champagne et al. [57] showed that $K_\psi \approx 0.64$. Sreenivasan [58] summarized many past results and argued that $K_\psi \approx 0.4$.

There are a number of papers on field theory of passive scalar turbulence. Here, we review only a couple of them for $d = 3$. Yakhot and Orszag [26] extended their RG computation (Section 4.1) to passive scalar and reported that $K_\psi = 1.16$. Zhou and Vahala [59] employed the recursive RG [see Section 4.2] to the scalar field, and reported that the turbulent Prandtl number ($\nu(k)/\kappa(k)$) is near 0.7. McComb et al. [60] employed *local energy transfer* (LET) theory (similar to recursive RG) and obtained $K_{\text{Ko}} = 2.5$ and $K_\psi = 1.1$. Antonov et al. [19] employed functional RG and reported that turbulent Prandtl number is 0.7040. Adzhemyan et al. [61] employed *operator product expansion* to compute anomalous scaling for the passive scalar turbulence (also see [53]). Verma [62] employed recursive RG and reported that the turbulent Prandtl number is 0.42, and $K_\psi = 1.25$.

The CH basis brings out the connections between the HDT and passive scalar turbulence quite nicely, which is described below. Since the scalar field does not affect the velocity field, $\nu_1^{(n)}$ follows the same equation as Eq. (89). We derive the renormalized diffusivity following the same procedure as that for u_2 (see Section 4.3). Figure 10 depicts the Feynman diagrams associated with the first-order perturbation of Eq. (125). The RG analysis yields

$$\kappa^{(n)} k^2 = \kappa^{(n+1)} k^2 - \text{Integrals corresponding to Fig. 10}, \quad (130)$$

or

$$\kappa^{(n)} k^2 = \kappa^{(n+1)} k^2 - \int^\Delta \frac{d\mathbf{p}}{(2\pi)^d} \left[\frac{kq C_1(\mathbf{p}) \sin \gamma \sin \alpha}{\nu_1(p) p^2 + \kappa(q) q^2} + \frac{kp C_1(\mathbf{q}) \sin \beta \sin \alpha}{\kappa(p) p^2 + \nu_1(q) q^2} \right], \quad (131)$$

where $C_1(\mathbf{p})$ is the spectral correlation for the u_1 component. Note that Eq. (131) has the same form as Eq. (88) with $\nu_2(k) \rightarrow \kappa(k)$.

The time scale for the scalar field (τ_k^ψ) is proportional to $(k u_k)^{-1}$. Therefore, we model $\kappa^{(n)}$ as [8, 62]

$$\kappa^{(n)} = \kappa_* \sqrt{K_{\text{Ko}}} \Pi^{1/3} k_n^{-4/3}, \quad (132)$$

which has the same form as Eq. (90), but with $\nu_{2*} \rightarrow \kappa_*$. Substitution of the above functions in the RG equation (131) yields

$$\kappa_*(1 - b^{-4/3}) = \frac{2S_{d-1}}{(d-1)S_d} \int_1^b p'^{d-1} dp' \int_{(p'^2+1-b^2)/(2p')}^{p'/2} dz (1-z^2)^{\frac{d-3}{2}} F_4(p', z),$$

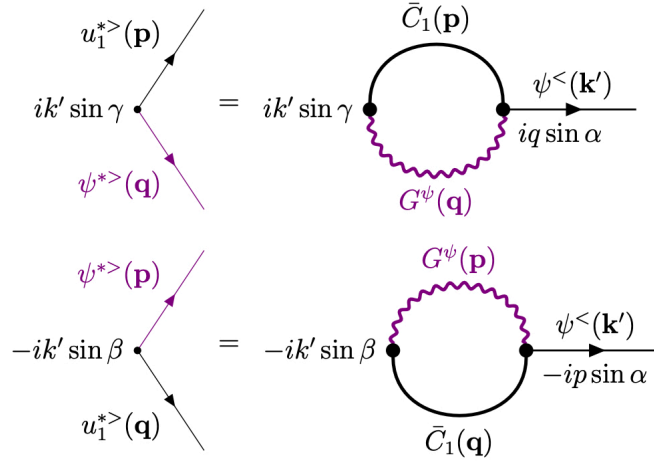


Fig. 10 Passive scalar turbulence: Feynman diagrams associated with the computation of renormalized diffusivity (κ). Here, $G^\psi(\mathbf{k})$ is the Green's function of the scalar field.

(133)

with

$$F_4(p', z) = \frac{(1-z^2)p'^{-2/3-d}}{\nu_{1*}p'^{2/3} + \kappa_*q'^{2/3}} + \frac{(1-z^2)p'^2q'^{-8/3-d}}{\kappa_*p'^{2/3} + \nu_{1*}q'^{2/3}}. \quad (134)$$

A comparison of Eq. (92) and Eq. (134) yields

$$\kappa_* = \nu_{2*}. \quad (135)$$

Hence, the renormalized κ and renormalized ν_2 are equal, both for 2D and 3D. Consequently, the turbulent Prandtl number

$$\frac{\nu_2(k)}{\kappa(k)} = \frac{\nu_{2*}}{\kappa_*} = 1. \quad (136)$$

Interestingly, the temporal evolution of passive scalar in 2D and u_z (velocity component perpendicular to the plane) in 2D3C are identical [see Eqs. (18, 125)]. Hence, their field theories are identical too.

Now, we compute the scalar energy flux using field theory. The mode-to-mode scalar energy transfer from $\psi(\mathbf{p})$ to $\psi(\mathbf{k}')$ with the mediation of $\mathbf{u}(\mathbf{q})$ is [62]

$$\langle S^{\psi\psi}(\mathbf{k}'|\mathbf{p}|\mathbf{q}) \rangle = -\Im[\langle \{\mathbf{k}' \cdot \mathbf{u}(\mathbf{q})\} \{\psi(\mathbf{p})\psi(\mathbf{k}')\} \rangle], \quad (137)$$

where $\mathbf{k}' + \mathbf{p} + \mathbf{q} = 0$. We compute the above triple correlation under quasi-Gaussian assumption. The Feynman diagram for the first-order perturbation, shown in Fig. 11,

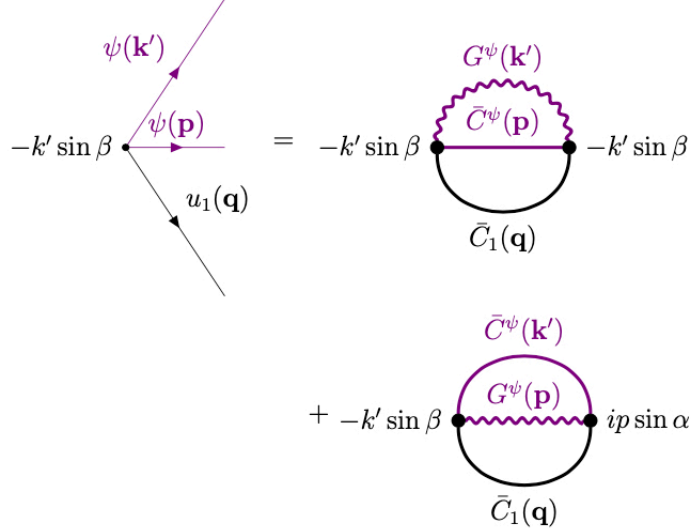


Fig. 11 Passive scalar turbulence: Feynman diagrams associated with the computation of mode-to-mode energy transfer ($\langle S^{\psi\psi}(\mathbf{k}'|\mathbf{p}|\mathbf{q}) \rangle$).

is similar to that for u_2 component in HDT (see Fig. 9). Following the procedure outlined in Section 5, we derive the following expression for $\langle S^{\psi\psi}(\mathbf{k}'|\mathbf{p}|\mathbf{q}) \rangle$:

$$\langle S^{\psi\psi}(\mathbf{k}'|\mathbf{p}|\mathbf{q}) \rangle = (k \sin \beta)^2 \frac{C_1(\mathbf{q})[C^{\psi}(\mathbf{p}) - C^{\psi}(\mathbf{k}')] }{\kappa(k)k^2 + \kappa(p)p^2 + \nu_1(q)q^2}, \quad (138)$$

or

$$\langle S^{\psi\psi}(v, z) \rangle = \frac{v^2 w^{-8/3-d} (v^{-2/3-d} - 1)(1 - z^2)}{\kappa_{2*}(1 + v^{2/3}) + \nu_{1*} w^{2/3}}, \quad (139)$$

where v, w are defined in Eq. (116).

Using the above mode-to-mode formula, we derive the corresponding scalar energy flux for a wavenumber sphere of radius R as

$$\langle \Pi_{\psi}(R) \rangle = \int_R^{\infty} \frac{d\mathbf{k}'}{(2\pi)^d} \int_0^R \frac{d\mathbf{p}}{(2\pi)^d} \langle S^{\psi\psi}(\mathbf{k}'|\mathbf{p}|\mathbf{q}) \rangle, \quad (140)$$

whose nondimensionalized version is

$$\frac{\langle \Pi_{\psi}(R) \rangle}{\Pi_{\psi}} = A_{\psi} \int_0^1 dv [\log(1/v)] v^{d-1} \int_{-1}^1 dz (1 - z^2)^{\frac{d-3}{2}} \langle S^{\psi\psi}(v, z) \rangle, \quad (141)$$

where

$$A_{\psi} = K_{\psi} K_{\text{Ko}}^{1/2} \frac{4}{(d-1)} \frac{S_{d-1}}{S_d}. \quad (142)$$

For $j = 2$, Eq. (121) has a similar form as Eq. (141) with $A \rightarrow A_\psi$ [see Eq. (122)]. Also note that $\langle \Pi_\psi(R) \rangle = \Pi_\psi$. Based on these observations, we derive that

$$K_\psi = \frac{K_{\text{Ko}}}{d-1} \quad (143)$$

The factor $d-1$ in Eq. (143) arises because $E^\psi(k)$ in Eq. (128) lacks the factor $d-1$ in comparison to Eq. (24). Equation (143) reveals that $K_\psi = K_{\text{Ko}}/2 \approx 0.8$ in 3D, which is consistent with Champagne et al. [57]'s conclusion that $K_\psi \approx 0.64$, but inconsistent with Sreenivasan [63]'s results. Verma [62] did not account for the $1/(d-1)$ factor correctly, which led to incorrect K_ψ . Interestingly, in 2D, the integral of Eq. (141) is positive, thus indicating a positive scalar energy flux despite inverse cascade of kinetic energy (in the $k^{-5/3}$ regime). Also, $K_\psi = K_{\text{Ko}}$ in 2D. These predictions need to be tested in future numerical simulations.

The above calculations demonstrate usefulness of CH basis in field theory. It provides a unified and transparent framework for HDT and passive scalar turbulence. In the next section, we employ field theory to MHD turbulence.

7 Field-theoretic Treatment of MHD Turbulence

Magnetohydrodynamics (MHD) is a description of quasi-neutral magnetized plasma at the continuum level [64]. In Fourier space, the MHD equations are [64]

$$\begin{aligned} \frac{d}{dt} \mathbf{u}(\mathbf{k}) + i \int \frac{d\mathbf{p}}{(2\pi)^d} \{\mathbf{k} \cdot \mathbf{u}(\mathbf{q})\} \mathbf{u}(\mathbf{p}) &= -ikp(\mathbf{k}) + i \int \frac{d\mathbf{p}}{(2\pi)^d} \{\mathbf{k} \cdot \mathbf{b}(\mathbf{q})\} \mathbf{b}(\mathbf{p}) \\ &\quad - \nu k^2 \mathbf{u}(\mathbf{k}) + \mathbf{f}(\mathbf{k}), \end{aligned} \quad (144)$$

$$\frac{d}{dt} \mathbf{b}(\mathbf{k}) + i \int \frac{d\mathbf{p}}{(2\pi)^d} \{\mathbf{k} \cdot \mathbf{u}(\mathbf{q})\} \mathbf{b}(\mathbf{p}) = i \int \frac{d\mathbf{p}}{(2\pi)^d} \{\mathbf{k} \cdot \mathbf{b}(\mathbf{q})\} \mathbf{u}(\mathbf{p}) - \eta k^2 \mathbf{b}(\mathbf{k}), \quad (145)$$

$$\mathbf{k} \cdot \mathbf{u}(\mathbf{k}) = 0, \quad (146)$$

$$\mathbf{k} \cdot \mathbf{b}(\mathbf{k}) = 0, \quad (147)$$

where \mathbf{u} , \mathbf{b} , and p are the velocity, magnetic, and pressure fields, respectively; ν and η are the kinematic viscosity and magnetic diffusivity, respectively; $\mathbf{k} = \mathbf{p} + \mathbf{q}$; and the external force \mathbf{f} is employed to the velocity field to maintain a steady state. In this review, we assume the mean magnetic field to be absent, which makes the flow statistically isotropic. We perform field-theoretic analysis using the Elsässer variables,

$$\mathbf{z}^\pm = \mathbf{u} \pm \mathbf{b}, \quad (148)$$

in terms of which the above MHD equations are

$$\frac{d}{dt} \mathbf{z}^\pm(\mathbf{k}) + i \int \frac{d\mathbf{p}}{(2\pi)^d} \{\mathbf{k} \cdot \mathbf{z}^\mp(\mathbf{q})\} \mathbf{z}^\pm(\mathbf{p}) = -ikp(\mathbf{k}) + \nu_+ k^2 \mathbf{z}^\pm(\mathbf{k}) + \nu_- k^2 \mathbf{z}^\mp(\mathbf{k}) + \mathbf{f}(\mathbf{k}), \quad (149)$$

$$\mathbf{k} \cdot \mathbf{z}^\pm(\mathbf{k}) = 0, \quad (150)$$

where $\nu_{\pm} = (\nu \pm \eta)/2$.

MHD turbulence has four nonlinear terms involving \mathbf{u} and \mathbf{b} fields that makes MHD turbulence more complex than HDT. There are several models of MHD turbulence, including anisotropic ones [35, 40, 65]. In this review, we focus on *isotropic MHD turbulence*, in particular on two competing turbulence phenomenologies whose spectral indices are 3/2 and 5/3 respectively. Kraichnan [66], Iroshnikov [67], and Dobrowolny et al. [68] argued that the energy spectra for the velocity and magnetic fields are equipartitioned with

$$E(k) = E^b(k) = K_{\text{Kr}}(\Pi_{\text{tot}}B_0)^{1/2}k^{-3/2}, \quad (151)$$

where $E(k), E^b(k)$ are the kinetic and magnetic energy spectra, respectively; Π_{tot} is the total energy flux (a sum of kinetic and energy fluxes); K_{Kr} is Kraichnan's constant; and B_0 is the mean magnetic field or an average amplitude of the large-scale magnetic fields.

Regarding the alternate phenomenology, Marsch [69] was the first to propose Kolmogorov-like turbulence phenomenology, according to which the energy spectra $E^{\pm}(k)$ for \mathbf{z}^{\pm} are (also see [40, 70])

$$E^{\pm}(k) = K^{\pm} \frac{(\Pi^{\pm})^{4/3}}{(\Pi^{\mp})^{2/3}} k^{-5/3}, \quad (152)$$

where Π^{\pm} are the energy fluxes for \mathbf{z}^{\pm} , and K^{\pm} are the respective constants. The spectral exponents 5/3 and 3/2 are quite close, and they are not easily differentiable in numerical simulations or in solar wind observations [40, 71, 72]. Various authors [70, 73–75] report one exponent or the other, thus making this issue inconclusive from the numerical perspective. In this section, we do not consider field theory of Kraichnan-Iroshnikov theory³. Instead, we focus on field theory of Kolmogorov-like turbulence phenomenology.

Leading field-theoretic works on MHD turbulence are as follows. Fournier et al. [76] generalized Forster et al. [27]'s framework to MHD turbulence, and predicted various scaling regimes as a function of space dimension d and the ratio of kinetic energy and magnetic energy. Adzhemyan et al. [77] performed similar calculations using quantum field theory renormalization group [53]. Goldreich and Sridhar [78] analyzed anisotropic MHD turbulence under strong turbulence limit, and showed that $E(k_{\perp}) \sim k_{\perp}^{-5/3}$ and $k_{\perp} z_{k_{\perp}} \sim k_{\parallel} B_0$, where k_{\perp}, k_{\parallel} are, respectively, the wavenumber components perpendicular and parallel to the mean magnetic field \mathbf{B}_0 . The latter relation is called *critical balance* [78]. Verma [40, 79–82] performed RG analysis of ν, η , and B_0 (mean magnetic field renormalization), as well as energy flux calculations for MHD turbulence; these calculations favor Kolmogorov-like turbulence phenomenology over Kraichnan-Iroshnikov phenomenology. Mizerski [83] employed RG to extract turbulent electromagnetic force for dynamo. A reader may also refer to reviews [40, 72].

In the following discussion, we illustrate RG and energy flux computations for a simplified version of MHD turbulence. Here, we work with \mathbf{z}^{\pm} variables and assume

³Kraichnan-Iroshnikov theory is discussed briefly in Section 8 in the framework of weak turbulence.

that

$$\langle E^+(k) \rangle = \langle E^-(k) \rangle, \quad (153)$$

$$\Re \langle [\mathbf{z}^+(\mathbf{k}) \cdot \mathbf{z}^{-*}(\mathbf{k})] \rangle = E^u(\mathbf{k}) - E^b(\mathbf{k}) = 0. \quad (154)$$

These assumptions simplify the algebra considerably. For this special case, the total energy (a sum of kinetic and magnetic energies) spectrum $E_{\text{tot}}(k) = E^+(k) = E^-(k)$, and

$$E_{\text{tot}}(k) = K \Pi_{\text{tot}}^{2/3} k^{-5/3}, \quad (155)$$

where $K = K^+ = K^-$ and $\Pi_{\text{tot}} = \Pi^+ = \Pi^-$ [40, 71]. Using $\tau_k^\pm \sim (kz_k^\mp)^{-1}$, we derive the respective renormalized diffusion coefficients as

$$\eta_\pm(k) = \eta_{\pm*} \sqrt{K^\mp} \frac{(\Pi^\mp)^{2/3}}{(\Pi^\pm)^{1/3}} k^{-4/3}. \quad (156)$$

For the special case discussed above, $\Pi^+ = \Pi^-$ and $\eta_+(k) = \eta_-(k)$.

As in HDT and passive scalar turbulence, CH basis simplifies the field-theoretic computations of MHD turbulence significantly. In the CH basis, the equations for $z_1^\pm(\mathbf{k}')$ and $z_2^\pm(\mathbf{k}')$ are given below:

$$\left(\frac{\partial}{\partial t} + \eta_1 k^2 \right) z_1^\pm(\mathbf{k}') = ik' \int \frac{d\mathbf{p}}{(2\pi)^d} [\sin \beta \cos \gamma z_1^{\mp*}(\mathbf{q}) z_1^{\pm*}(\mathbf{p}) - \sin \gamma \cos \beta z_1^{\mp*}(\mathbf{p}) z_1^{\pm*}(\mathbf{q})] + f_1(\mathbf{k}'), \quad (157)$$

$$\left(\frac{\partial}{\partial t} + \eta_2 k^2 \right) z_2^\pm(\mathbf{k}') = ik' \int \frac{d\mathbf{p}}{(2\pi)^d} \{ \sin \gamma z_1^{\mp*}(\mathbf{p}) z_2^{\pm*}(\mathbf{q}) - \sin \beta z_1^{\mp*}(\mathbf{q}) z_2^{\pm*}(\mathbf{p}) \} + f_2(\mathbf{k}'). \quad (158)$$

As in HDT, we assume different diffusive coefficients for z_1 and z_2 components as follows:

$$\eta_{1+} = \eta_{1-} = \eta_1, \quad (159)$$

$$\eta_{2+} = \eta_{2-} = \eta_2. \quad (160)$$

To compute the renormalized $\eta_{1,2}$, we expand the nonlinear terms of Eqs. (157, 158) to first order (as in Section 4.3). The corresponding Feynman diagrams are shown in Figs. 12 and 13 that yield the following recurrence relations for the renormalized η_1 and η_2 :

$$\eta_1^{(n)} k^2 = \eta_1^{(n+1)} k^2 + \int_{\Delta} \frac{d\mathbf{p}}{(2\pi)^d} \frac{1}{\nu_1(p)p^2 + \nu_1(q)q^2} [kp \sin \beta \sin \alpha \cos^2 \gamma C_1^-(\mathbf{q}) + kq \sin \beta \sin \gamma \cos^2 \beta C_1^-(\mathbf{p})], \quad (161)$$

$$\eta_2^{(n)} k^2 = \eta_2^{(n+1)} k^2 + \int_{\Delta} \frac{d\mathbf{p}}{(2\pi)^d} \left[\frac{kq C_1^-(\mathbf{p}) \sin \gamma \sin \alpha}{\eta_1(p)p^2 + \eta_2(q)q^2} + \frac{kp C_1^-(\mathbf{q}) \sin \beta \sin \alpha}{\eta_2(p)p^2 + \eta_1(q)q^2} \right] \quad (162)$$

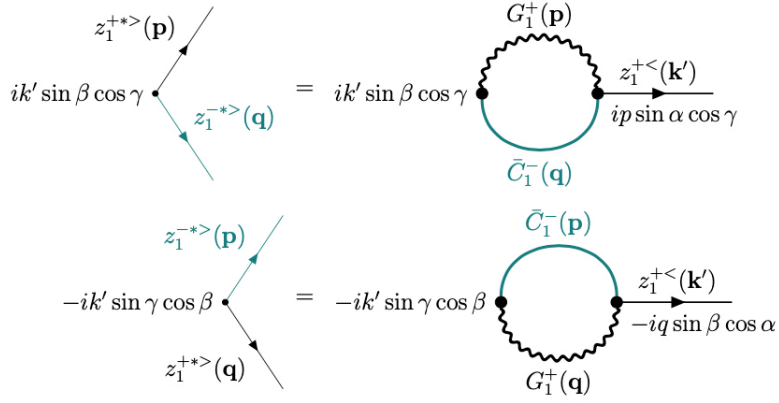


Fig. 12 MHD turbulence: Feynman diagrams associated with the computation of renormalized diffusivity η_1 .

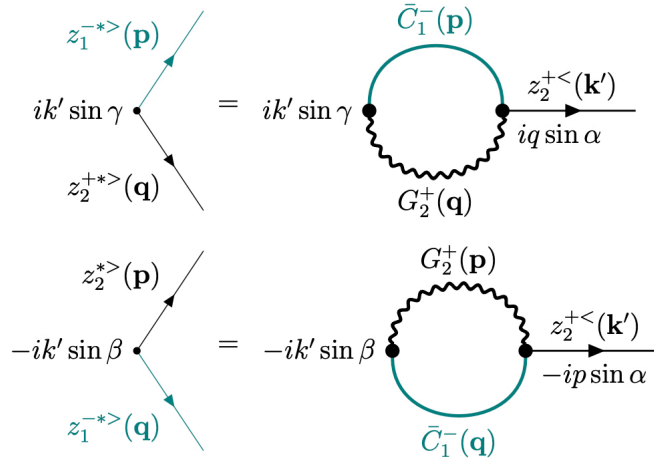


Fig. 13 MHD turbulence: Feynman diagrams associated with the computation of renormalized diffusivity η_2 .

Note that $C_1^+ = C_1^- = C_1$ because of Eq. (153). Also, the vanishing of the cross terms in Eq. (154) help remove some other terms. Thus, Eqs. (153, 154) simplify the RG equations considerably.

Following similar steps as for HDT (Section 4.3), we derive that

$$\eta_{(1,2)*}(1 - b^{-4/3}) = \frac{2S_{d-1}}{(d-1)S_d} \int_1^b p'^{d-1} dp' \int_{(p'^2+1-b^2)/(2p')}^{p'/2} dz (1-z^2)^{\frac{d-3}{2}} F_{(5,6)}(p', z),$$

(163)

where

$$F_5(p', z) = \frac{(1-z^2)z^2 p'^2 q'^{-8/3-d}}{\eta_{1*} p'^{2/3} + \eta_{1*} q'^{2/3}} + \frac{(1-z^2)(1-p'z)^2 p'^{-8/3-d}/w^2}{\eta_{1*} p'^{2/3} + \eta_{1*} q'^{2/3}}, \quad (164)$$

$$F_6(p', z) = \frac{(1-z^2)p'^{-2/3-d}}{\eta_{1*} p'^{2/3} + \eta_{2*} q'^{2/3}} + \frac{(1-z^2)p'^2 q'^{-8/3-d}}{\eta_{2*} p'^{2/3} + \eta_{1*} q'^{2/3}}. \quad (165)$$

The integrals of Eq. (163) converge for both 2D and 3D. For the RG parameter $c = 1.5$, $\eta_{1*} = 0.22$ and $\eta_{2*} = 0.50$ for 2D, and $\eta_{1*} = 0.19$ and $\eta_{2*} = 0.48$ for 3D.

After this, we compute the energy fluxes for \mathbf{z}^\pm using the following formulae:

$$S^{z_1 z_1}(\mathbf{k}'|\mathbf{p}|\mathbf{q}) = k' \sin \beta \cos \gamma \Im\{z_1^-(\mathbf{q})z_1^+(\mathbf{p})z_1^+(\mathbf{k}')\}, \quad (166)$$

$$S^{z_2 z_2}(\mathbf{k}'|\mathbf{p}|\mathbf{q}) = -k' \sin \beta \Im\{z_1^-(\mathbf{q})z_2^+(\mathbf{p})z_2^+(\mathbf{k}')\}. \quad (167)$$

Since $\langle E^+(k) \rangle = \langle E^-(k) \rangle$, \mathbf{z}^+ and \mathbf{z}^- channels have the same energy transfers statistically. The above energy transfers vanish to the zeroth order. Hence, we expand $S^{z_1 z_1}(\mathbf{k}'|\mathbf{p}|\mathbf{q})$ and $S^{z_2 z_2}(\mathbf{k}'|\mathbf{p}|\mathbf{q})$ to first order that yields Feynman diagrams shown in Figs. 14 and 15 and the following formulas:

$$\langle S^{z_1 z_1}(\mathbf{k}'|\mathbf{p}|\mathbf{q}) \rangle = (k \sin \beta)^2 (\cos \gamma)^2 \frac{C_1^-(\mathbf{q})[C_1^-(\mathbf{p}) - C_1^-(\mathbf{k}')] }{\eta_1(k)k^2 + \eta_1(p)p^2 + \eta_1(q)q^2}, \quad (168)$$

$$\langle S^{z_2 z_2}(\mathbf{k}'|\mathbf{p}|\mathbf{q}) \rangle = (k \sin \beta)^2 \frac{C_1^-(\mathbf{q})[C_2^-(\mathbf{p}) - C_2^-(\mathbf{k}')] }{\eta_2(k)k^2 + \eta_2(p)p^2 + \eta_1(q)q^2}. \quad (169)$$

For 2D, the energy flux $\Pi(R)$ is

$$\langle \Pi(R) \rangle = \langle \Pi^+(R) \rangle = \langle \Pi^-(R) \rangle = \int_R^\infty \frac{d\mathbf{k}'}{(2\pi)^d} \int_0^R \frac{d\mathbf{p}}{(2\pi)^d} \langle S^{z_1 z_1}(\mathbf{k}'|\mathbf{p}|\mathbf{q}) \rangle. \quad (170)$$

Following similar steps as in Sec. 5.2, we derive the constant $K^+ = K^- = K = 0.85$ for 2D MHD turbulence. The above relation also indicates that the energy cascades for \mathbf{z}^\pm are positive in 2D, consistent with the absolute equilibrium theory for MHD turbulence [14, 84]. This is in contrast to 2D HDT that exhibits inverse energy cascade. For 3D MHD turbulence,

$$\langle \Pi(R) \rangle = \langle \Pi^+(R) \rangle = \langle \Pi^-(R) \rangle = \int_R^\infty \frac{d\mathbf{k}'}{(2\pi)^d} \int_0^R \frac{d\mathbf{p}}{(2\pi)^d} [\langle S^{z_1 z_1}(\mathbf{k}'|\mathbf{p}|\mathbf{q}) \rangle + \langle S^{z_2 z_2}(\mathbf{k}'|\mathbf{p}|\mathbf{q}) \rangle]. \quad (171)$$

After the integral computation, we obtain $K^+ = K^- = K = 0.96$ for 3D.

In MHD turbulence, we can vary various parameters: $E^+(k)/E^-(k)$, $E(k)/E_b(k)$, and $\Re[\mathbf{u}(\mathbf{k}) \cdot \mathbf{b}^*(\mathbf{k})]$, whose variations lead to significant changes in the turbulence properties, including K^\pm and Π^\pm . This is possibly the reason why our field-theoretic results on K^\pm differ from the past works. For example, in 3D, for $\langle E^+(k) \rangle = \langle E^-(k) \rangle$

$$\begin{aligned}
& \begin{array}{c} z_1^+(\mathbf{k}') \\ | \\ k' \sin \beta \cos \gamma \text{ --- } z_1^+(\mathbf{p}) \\ | \\ z_1^-(\mathbf{q}) \end{array} = k' \sin \beta \cos \gamma \begin{array}{c} G_1^+(\mathbf{k}') \\ \text{---} \text{---} \text{---} \\ \bar{C}_1^+(\mathbf{p}) \\ \text{---} \text{---} \text{---} \\ \bar{C}_1^-(\mathbf{q}) \end{array} ik' \sin \beta \cos \gamma \\
& + k' \sin \beta \cos \gamma \begin{array}{c} \bar{C}_1^+(\mathbf{k}') \\ \text{---} \text{---} \text{---} \\ G_1^+(\mathbf{p}) \\ \text{---} \text{---} \text{---} \\ \bar{C}_1^-(\mathbf{q}) \end{array} -ip \sin \alpha \cos \gamma
\end{aligned}$$

Fig. 14 MHD turbulence: Feynman diagrams associated with the computation of mode-to-mode energy transfer via $z_1 z_1$ channel ($\langle S^{z_1 z_1}(\mathbf{k}'|\mathbf{p}|\mathbf{q}) \rangle$).

$$\begin{aligned}
& \begin{array}{c} z_2^+(\mathbf{k}') \\ | \\ -k' \sin \beta \text{ --- } z_2^+(\mathbf{p}) \\ | \\ z_1^-(\mathbf{q}) \end{array} = -k' \sin \beta \begin{array}{c} G_2^+(\mathbf{k}') \\ \text{---} \text{---} \text{---} \\ \bar{C}_2^+(\mathbf{p}) \\ \text{---} \text{---} \text{---} \\ \bar{C}_1^-(\mathbf{q}) \end{array} -ik' \sin \beta \\
& + -k' \sin \beta \begin{array}{c} \bar{C}_2^+(\mathbf{k}') \\ \text{---} \text{---} \text{---} \\ G_2^+(\mathbf{p}) \\ \text{---} \text{---} \text{---} \\ \bar{C}_1^-(\mathbf{q}) \end{array} ip \sin \alpha
\end{aligned}$$

Fig. 15 MHD turbulence: Feynman diagrams associated with the computation of mode-to-mode energy transfer via $z_2 z_2$ channel ($\langle S^{z_2 z_2}(\mathbf{k}'|\mathbf{p}|\mathbf{q}) \rangle$).

and $\langle E(k)/E_b(k) \rangle \approx 0.7$, Verma [40]’s field theory work yields $K^+ \approx K^- \approx 1.5$. Using numerical simulations, Beresnyak [75] reported that the Kolmogorov’s constant lies between 3.2 to 4.2 depending on Alfvénicity. Note that $\langle E^+(k) \rangle = \langle E^-(k) \rangle$ and/or $\langle E(k) \rangle = \langle E_b(k) \rangle$ differ for these works. We need to carefully compare the field-theoretic and numerical results for various cases. However, we do not delve into these details in this review.

In Section 8 we discuss field theory of weak turbulence.

8 Field Theory of Weak Turbulence

In HDT, scalar turbulence, and MHD turbulence, we compute the renormalized diffusive parameters and energy fluxes using field theory. In such flows, the nonlinearity dominates the linear term, which is not the case for some other systems, for example, weakly nonlinear water waves, strongly rotating flow, MHD with strong \mathbf{B}_0 , etc. For the latter kind of systems, we do not renormalize the parameter(s), but compute the energy fluxes. The energy spectrum is deduced using the energy flux formula. Such a framework is called *weak turbulence* [85–87]. In this section, we will briefly illustrate this framework and apply it to the *advection equation*.

8.1 Weak Turbulence Framework

Zakharov et al. [85] extended the quantum field theory formalism to weak turbulence. We illustrate this framework starting with Schrödinger equation:

$$i\partial_t\psi = (H_0 + H_1)\psi, \quad (172)$$

where ψ is the wavefunction, and H_0 and H_1 are the bare (unperturbed) and perturbed parts of the Hamiltonian, respectively. Here, we set the Planck constant $\hbar = 1$. Zakharov assumed H_1 to be a nonlinear function of ψ , and that $\|H_1\| \ll \|H_0\|$. As an example, we consider

$$H_0\psi(\mathbf{k}) = \hbar\omega(\mathbf{k})\psi(\mathbf{k}); \quad H_1\psi = -\nabla^2\psi^3. \quad (173)$$

In Fourier space, Eqs. (172, 173) transform to the following:

$$i\partial_t\psi(\mathbf{k}, t) = \omega(\mathbf{k})\psi(\mathbf{k}, t) + k^2 \int \frac{d\mathbf{p}}{(2\pi)^d} \frac{d\mathbf{q}}{(2\pi)^d} \psi(\mathbf{p}, t)\psi(\mathbf{q}, t)\psi(\mathbf{s}, t), \quad (174)$$

where $\mathbf{s} = \mathbf{k} - \mathbf{p} - \mathbf{q}$. Here, the nonlinearity is cubic; it comes in different order in other systems.

Using Eq. (174) we derive the following equation for the particle density $\langle |\psi(\mathbf{k}, t)|^2 \rangle$:

$$\partial_t \frac{1}{2} \langle |\psi(\mathbf{k}, t)|^2 \rangle = k^2 \Im \left[\int \frac{d\mathbf{p}}{(2\pi)^d} \frac{d\mathbf{q}}{(2\pi)^d} \langle \psi(\mathbf{p}, t)\psi(\mathbf{q}, t)\psi(\mathbf{s}, t)\psi^*(\mathbf{k}, t) \rangle \right] = T_N(\mathbf{k}, t), \quad (175)$$

where $T_N(\mathbf{k}, t)$ is the nonlinear particle transfer term⁴. Note that the linear term vanishes in Eq. (175). Following the discussion of Sec. 5.2, we deduce the following formula for the particle flux $\Pi_N(R)$ for a wavenumber sphere of radius R :

$$\Pi_N(R) = - \int \frac{d\mathbf{k}'}{(2\pi)^d} T_N(\mathbf{k}'); \quad (176)$$

$\Pi_N(R)$ is interpreted as the rate of particle transfer for a wavenumber of radius R . Similar formula can be constructed for the energy flux.

In a conservative or isolated system [e.g., in Eq. (172)], the total number of particles $[\int d\mathbf{k} |\psi(\mathbf{k}, t)|^2]$ is conserved, and a wavenumber sphere of radius R contains a finite number of particles. Therefore, a *steady* particle flux from this sphere is impossible because this flux will deplete the particles in the sphere in a finite time. Finite $\Pi_N(R)$ is possible only when the particles are constantly injected into the system, which is a nonequilibrium and open framework. Weak turbulence framework assumes energy and particle injections by an external source (e.g., electromagnetic or mechanical forcing for Bose-Einstein condensate [88]) and dissipation at small scales. We will illustrate a detailed calculation of weak turbulence in the next subsection. It is important to emphasize that a typical isolated or conservative system *thermalizes or reaches equilibrium* asymptotically; that is, the energy and particles are evenly distributed among all the Fourier modes. A quantum system may approach Fermi-Dirac or Bose-Einstein statistics asymptotically depending on the particle nature.

Next, we apply wave turbulence theory to the advection equation.

8.2 Application of Weak Turbulence to Advection Equation

The advection equation for a scalar field ϕ is

$$\partial_t \phi + V \partial_x \phi = -\partial_x \frac{\phi^2}{2}, \quad (177)$$

where V is the advection speed. Here, we assume that the advection term, $V \partial_x \phi$ dominates the nonlinear term, $-\partial_x \phi^2/2$. The equation for the modal scalar energy is

$$\partial_t \frac{1}{2} \langle |\phi(\mathbf{k}, t)|^2 \rangle = T(\mathbf{k}, t) = \frac{k_x}{2} \int \frac{d\mathbf{p}}{(2\pi)^d} \Im \langle \phi(\mathbf{p}, t) \phi(\mathbf{q}, t) \phi^*(\mathbf{k}, t) \rangle, \quad (178)$$

where $\mathbf{k} = \mathbf{p} + \mathbf{q}$, and $T(\mathbf{k}, t)$ is the transfer term for the scalar energy. Note the advection term is cancelled out in Eq. (178). In addition, the Green's function and the unequal-time correlation function for the unperturbed advection equation are

$$G(\mathbf{k}, t - t') = H(t - t') \exp[-ik_x V(t - t')], \quad (179)$$

$$\bar{C}(\mathbf{k}, t - t') = C(\mathbf{k}) \exp[-ik_x V(t - t')], \quad (180)$$

⁴A typical weak turbulence calculation employs $\psi(\mathbf{k}, t) = a(\mathbf{k}, t) \exp(-i\omega(\mathbf{k})t)$, as in the interaction picture of quantum mechanics. We avoid this extra step in our derivation.

where $C(\mathbf{k})$ is the equal-time correlation function (assumed to be a steady function), and $H(t - t')$ is the heaviside function. Note that V is not renormalized because the nonlinear term is much weaker than advection term.

In this review, we compute $T(\mathbf{k}, t)$ using the procedure of Sec. 5.2. An expansion of Eq. (178) to first-order yields Feynman diagrams similar to Fig. 8. The energy transfer term corresponding to the first Feynman diagram of Fig. 8 is

$$\begin{aligned} T_1(\mathbf{k}, t) &= \Im \left\{ \frac{ik_x^2}{4} \int \frac{d\mathbf{p}}{(2\pi)^d} \int_0^t dt' G(\mathbf{k}, t - t') \bar{C}(\mathbf{p}, t - t') \bar{C}(\mathbf{q}, t - t') \right\} \\ &= \Im \left\{ \frac{ik_x^2}{4} \int \frac{d\mathbf{p}}{(2\pi)^d} \frac{C(\mathbf{p})C(\mathbf{q})}{[-iV(k_x - p_x - q_x) + \epsilon]} \right\} \\ &= \frac{\pi k_x^2}{4V} \int \frac{d\mathbf{p}}{(2\pi)^d} \delta(k_x - p_x - q_x) C(\mathbf{p})C(\mathbf{q}), \end{aligned} \quad (181)$$

where ϵ is a small parameter that induces dissipation at small scales [85]. In the last step, we employed *Cauchy principal value theorem*:

$$\frac{1}{x + i\epsilon} = P\left(\frac{1}{x}\right) - i\pi\delta(x), \quad (182)$$

where $P(1/x)$ is the Cauchy principal value. Following similar steps for the other two Feynman diagrams, we obtain

$$T(\mathbf{k}, t) = \frac{\pi k_x}{4V} \int \frac{d\mathbf{p}}{(2\pi)^d} \delta(k_x - p_x - q_x) [k_x C(\mathbf{p})C(\mathbf{q}) - p_x C(\mathbf{q})C(\mathbf{k}) - q_x C(\mathbf{p})C(\mathbf{k})]. \quad (183)$$

The next task is to compute the inertial-range energy flux, which is

$$\Pi(k) = - \int_0^k \frac{dk'}{(2\pi)^d} T(\mathbf{k}', t). \quad (184)$$

The above integral is quite complex with significant anisotropy. Zakharov transformation [85] is often used to simplify the flux integration. I avoid the computation details in this short review. Instead, I simplify the calculation by assuming isotropy, $p_x \rightarrow p$, and $C(\mathbf{p}) \sim E(p)/p^{d-1}$. In addition, as is customary in weak turbulence, I assume *locality*, according to which wavenumbers with near magnitudes interact ($k \approx p \approx q$), leading to $C(k') \approx C(p) \approx C(q)$ [85]. Therefore,

$$\Pi(k) = \frac{k^2}{V} k^d k^{d-1} \left(\frac{E(k)}{k^{d-1}} \right)^2. \quad (185)$$

Hence, for a constant $\Pi(k) = \Pi$,

$$E(k) \sim (\Pi V)^{1/2} k^{-3/2}. \quad (186)$$

Thus, the scalar energy spectrum for the advection equation is $k^{-3/2}$ (not $k^{-5/3}$).

Interestingly, for MHD turbulence with strong \mathbf{B}_0 , Kraichnan [66] and Iroshnikov [67] argued that the advection of Alfvén waves by \mathbf{B}_0 via $\mathbf{B}_0 \cdot \nabla \mathbf{z}^\pm$ dominates the nonlinear terms, where \mathbf{z}^\pm are the amplitudes of the Alfvén waves in terms of Elsässer variables. For $\mathbf{B}_0 = B_0 \hat{x}$,

$$\mathbf{B}_0 \cdot \nabla \mathbf{z}^\pm = B_0 \partial_x \mathbf{z}^\pm, \quad (187)$$

which has a similar form as the advection term in Eq. (177). Multiple fields (\mathbf{z}^\pm) and different resonant conditions make the weak MHD turbulence more complex than advection equation. Still, following the derivation outlined in this subsection, we can derive that $E(k) \sim k^{-3/2}$ [67, 86]. A more sophisticated derivation by Galtier et al. [89] yields $E(k_\perp) \sim k_\perp^{-2}$; this derivation, however, is beyond the scope of this review.

8.3 Sweeping Effect and $k^{-3/2}$ Spectrum

Section 8.2 is a gist of Kraichnan’s arguments for the $k^{-3/2}$ spectrum for HDT [90]. Note, however, that Kraichnan [90] assumed the advection speed V to be random, which leads to

$$G(\mathbf{k}, t - t') = H(t - t') \langle \exp[-i\mathbf{k} \cdot \mathbf{V}(t - t')] \rangle = H(t - t') \exp[-\frac{1}{2} V^2 k^2 (t - t')], \quad (188)$$

$$\bar{C}(\mathbf{k}, t - t') = C(\mathbf{k}) \langle \exp[-i\mathbf{k} \cdot \mathbf{V}(t - t')] \rangle = C(\mathbf{k}) \exp[-\frac{1}{2} V^2 k^2 (t - t')], \quad (189)$$

substitution of which in Eq. (181) yields Eq. (186), albeit with a slightly more complex dt' integral in Eq. (181). Here, an advection of fluctuations by V (*random* mean flow or large-scale eddies) yields $k^{-3/2}$ spectrum in Eulerian framework, which is inconsistent with the experimental observations of $k^{-5/3}$ spectrum. Based on this result, Kraichnan [90] argued that Eulerian approach is inappropriate for the field-theoretic treatment of HDT. Later, Kraichnan went on to create Lagrangian-based field theory, e.g., *Mixed Lagrangian-Eulerian approach* [22], *Lagrangian-History Closure Approximation* [23], *Test Field Model* [24], etc., to derive $k^{-5/3}$ energy spectrum for HDT. These theories, however, are beyond the scope of this review. We refer a reader to Kraichnan’s original papers and Leslie [9].

In spite of above warnings by Kraichnan, Eulerian framework has been successfully employed in a large number of field theory calculations of hydrodynamic, scalars, and MHD turbulence (see Sections 4, 5, 6, 7). So, how do we reconcile Kraichnan’s objections with the success of Eulerian field theory? Our viewpoint on this topic is as follows. Verma et al. [91] performed RG analysis of the following equations:

$$\frac{\partial \mathbf{u}}{\partial t} - \nu \nabla^2 \mathbf{u} = -\mathbf{U}_0 \cdot \nabla \mathbf{u} - \mathbf{u} \cdot \nabla \mathbf{u} - \nabla p + \mathbf{f}, \quad (190)$$

$$\nabla \cdot \mathbf{u} = 0, \quad (191)$$

where \mathbf{U}_0 is the mean velocity field. The steps of the RG computations remain the same as in Section 4, except that the small frequency limit of Eq. (54) is replaced by

the Doppler-shifted frequency $\omega_D = \omega - \mathbf{U}_0 \cdot \mathbf{k} \rightarrow 0$. These steps yield $k^{-5/3}$ energy spectrum and the same renormalized viscosity as in Sec. 4. Thus, Verma et al. [91] showed that the renormalized parameters and energy spectrum remain unchanged with \mathbf{U}_0 , which is consistent with Galilean invariance. However, random fluctuations at large scales do affect the correlations [91–93], as we describe below.

The *sweeping effect* is apparent in numerical $\bar{C}(\mathbf{k}, t - t')$. Using numerical data of isotropic HDT, it has been shown that $\bar{C}(\mathbf{k}, t - t')$ follows the following form [91–93]:

$$\frac{\bar{C}(\mathbf{k}, t - t')}{C(\mathbf{k})} = \exp[-\nu(k)k^2(t - t')] \exp[-ick\tilde{U}_0(t - t')] \exp[-i\mathbf{U}_0 \cdot \mathbf{k}(t - t')], \quad (192)$$

where \mathbf{U}_0 is the mean velocity field, and \tilde{U}_0 is the random large-scale velocity. In Eq. (192), $\exp[-i\mathbf{U}_0 \cdot \mathbf{k}(t - t')]$ is the trivial advection term that is related to Taylor's frozen-in hypothesis [94], whereas $\exp[-ick\tilde{U}_0(t - t')]$ represents sweeping effect by random large-scale velocity. Verma et al. [91] argued that $k\tilde{U}_0 \sim k^{2/3}$ will yield $k^{-5/3}$ energy spectrum even in the presence of random sweeping effect; this hypothesis however needs to be tested using high-resolution simulations. In addition, it will be interesting to attempt a RG calculation for ν and \tilde{U}_0 simultaneously. Thus, sweeping effect remains an enigma even after 60 years of research.

In addition, weak turbulence theory has been applied to many other systems, including anisotropic ones. However, we do not discuss this topic any further due to lack of space. Next, we will briefly discuss field theory of intermittency.

9 Field Theory for Intermittency

In equilibrium field theory, n -th order correlation functions and the respective Green's functions are the same, and they have been computed for various systems in the past [1–3]. However, the Green's function and the correlation function are different in nonequilibrium field theory, turbulence being one of them [e.g., see Eqs. (34, 35)]. In turbulence field theory, the second-order and triple-order correlations of the velocity field have been computed by many researchers.

Kolmogorov [6, 7] derived the exact third-order structure function under the assumption of homogeneity and isotropy [see Eq. (4)]. Note that Eqs. (4, 109) yield average energy flux Π . However, the fluctuations in Π have not been computed from the first principle. Similarly, no one has been able to derive higher-order correlations for \mathbf{u} in HDT from the first principles.

The q -th order structure function is defined as [20]

$$S_q(l) = \left\langle |(\mathbf{u}(\mathbf{x} + \mathbf{l}) - \mathbf{u}(\mathbf{x})) \cdot \hat{l}|^q \right\rangle, \quad (193)$$

where $q > 0$, often taken as integers from 1 to 10 or so. Phenomenologically,

$$S_q(l) = \left\langle \Pi_l^{q/3} \right\rangle l^{q/3}, \quad (194)$$

where Π_l denotes the fluctuating energy flux at length scale l . Note that

$$\langle \Pi_l \rangle = \Pi, \quad \text{but} \quad \langle \Pi_l^q \rangle \neq \Pi^q \quad (195)$$

because of the nontrivial probability distribution of Π_l . In literature, the fluctuations in Π_l has been modelled as [20]

$$\langle \Pi_l^q \rangle = A_q \langle \Pi \rangle^q \left(\frac{l}{L} \right)^{\tau_q}, \quad (196)$$

where A_q 's are constants, and τ_q 's are exponents related to the energy flux. Substitution of Eq. (196) in Eq. (194) yields [20]

$$S_q(l) = A_{q/3} \langle \Pi \rangle^{q/3} l^{q/3 + \tau_{q/3}} L^{-\tau_{q/3}} = A_{q/3} \langle \Pi \rangle^{q/3} l^{\zeta_q} L^{-\tau_{q/3}}, \quad (197)$$

where

$$\zeta_q = q/3 + \tau_{q/3} \quad (198)$$

is called the *intermittency exponent*. A simple generalization of Kolmogorov's theory yields $\zeta_q = q/3$, which is inconsistent with the numerical and experimental observations [20]. Researchers have constructed various phenomenological models, e.g., *fractal model* [95], *lognormal model* [96], *multifractal model* [97], *She-Leveque model* [98]. Among them, She-Leveque model [98] provides the best fit to the numerical and experimental observations. Note, however, that the above models are not first-principle computations from the NS equation.

In the following, we briefly describe several field-theoretic attempts to compute the intermittency exponents.

1. Belinicher et al. [99] developed a field-theoretic procedure to compute the intermittency exponent ζ_q . In a series of follow-up papers, L'vov and Procaccia [100, 101, 102] derived scaling relations among the intermittency exponents using exact resummation of all the Feynman diagrams. These computations are divergence-free in infrared and ultraviolet regimes. The above scaling relations, referred to as *fusion rules* [33, 103], are in good agreement with the experimental results of atmospheric turbulence.
2. Onsager [104], Frisch [20], and Eyink and Sreenivasan [18] discussed *Euler singularity* and *dissipative anomaly*. Note that infinitesimal ν yields a finite energy dissipation or flux, whereas zero viscosity in spectrally-truncated Euler turbulence leads to an equilibrium solution with no energy flux. Migdal [105] investigated the inviscid limit of the Navier-Stokes equation and reported anomalous terms in Hamiltonian, dissipation, and helicity. Migdal and collaborators also proposed *area law* for HDT. These issues have been partially addressed by mathematicians [106] and field theorists [105, 107], but final word is not yet out.
3. *Functional renormalization* and *generating functionals* have been employed to compute correlation functions to all orders, both in equilibrium [1] and nonequilibrium settings [19, 30, 47]. The equilibrium computations have been quite successful, but the intermittency exponents computed using nonequilibrium framework differ from

the experimental and numerical results [47]. Interestingly, Moriconi [108] calculated the statistics of intense turbulent vorticity events using Martin-Siggia-Rose functional framework; these results are in good agreement with numerical simulations. These computations are quite complex, and they are beyond the scope of this paper.

4. Das and Bhattacharjee [109] employed mode coupling method to compute the second-order correlation for the energy flux, $\langle \Pi(\mathbf{x})\Pi(\mathbf{x} + \mathbf{l}) \rangle$. A generalization of the above computation to higher orders may yield statistics on the fluctuations in Π_l , which is a crucial factor in modelling intermittency.
5. Intermittency exponents have been computed exactly for the passive scalar turbulence with the advective velocity field correlated in space, but delta-correlated in time (given by Kraichnan model) [34]. These calculations, based on semi-Lagrangian field-theoretic approach, are quite complex. A reader may refer to the original papers cited in the review article [34]. There have been attempts to generalize these calculations to HDT, but they have been unsuccessful so far.

In the next section, I compare turbulence field theory with other field theories.

10 Comparing Turbulence with Other Field Theories

From a dynamical perspective, field theories are broadly classified into the following three categories.

1. *Equilibrium field theories* describe systems in equilibrium with heat bath (in classical field theory) or with quantum noise (in quantum field theory). Examples of such field theories include Ising model, Wilson's ϕ^4 theory, and Hubbard model. Here, the fields are Gaussian or quasi-Gaussian, and they respect detailed balance. The Green's and correlation functions are the same in these field theories.

It is conjectured that isolated multi-particle systems (both classical and quantum) thermalize asymptotically [110]. In turbulence, spectrally-truncated Euler equation ($\nu = 0$) and Gross-Pitaevskii (GP) equation with zero potential are isolated systems that thermalize asymptotically [5, 86, 111]. Typically, these systems exhibit equipartition of energy or particles among the available Fourier modes, and zero energy or particle flux (see Sections 4 and 5). Researchers have invoked several mechanisms, including *Berry's conjecture* [112], to explain thermalization. In turbulence, the forward energy flux from large scales to small scales plays a key role in the redistribution of energy towards thermalization. Verma [113, 114] has argued that the energy flux may work as a thermalization mechanism in isolated multi-particle systems.

It is known that several quantum systems do not thermalize, with prime examples being *many body localization* [115] and *time crystals* [116]. For many body localization, emergent integrability and multiple conserved quantities are believed to be the key factors for nonthermalization [115]. Interestingly, 2D Euler turbulence does not thermalize for some ordered initial condition, possibly due to its multiple conserved quantities [117]. Thus, 2D Euler turbulence and many body localization appear to share several common features. This issue needs further exploration.

2. *Near-equilibrium systems* are out of equilibrium, but they are quite close to equilibrium. A popular example is thermal conduction where the directional heat transport breaks detailed balance. Systems near equilibrium obey *fluctuation-dissipation theorem* [118]. To illustrate, for the diffusion equation,

$$\partial_t \phi(\mathbf{k}, t) = -\kappa k^2 \phi(\mathbf{k}, t) + f_\phi(\mathbf{k}, t), \quad (199)$$

where f_ϕ is the white noise, the Green's function is

$$G(\mathbf{k}, t - t') = H(t - t') \exp[-\kappa k^2(t - t')], \quad (200)$$

with $H(t - t')$ as the step function. For this system, the fluctuation-dissipation theorem yields

$$|\phi(\mathbf{k}, \omega)|^2 = C(\mathbf{k}, \omega) = \frac{k_B T}{\omega} \Im[G(\mathbf{k}, \omega)], \quad (201)$$

or

$$C(\mathbf{k}, t - t') = C(\mathbf{k}) \exp[-\kappa k^2(t - t')], \quad (202)$$

where

$$C(\mathbf{k}) = |f_\phi(\mathbf{k}, t)|^2 = k_B T \quad (203)$$

is the equipartitioned thermal energy of each Fourier mode. Note that the fluctuation-dissipation theorem tells us how the correlation function $C(\mathbf{k}, t - t')$ and Green's function $G(\mathbf{k}, t - t')$ decay with time.

3. *Nonequilibrium field theories* describe systems that are far from equilibrium. A typical nonequilibrium system has an external driving at large scales and dissipation at small scales. Some prominent examples are turbulence [8], *active matter* [119], *coarsening systems* [45, 120], and *driven quantum turbulence* (e.g., *superfluids*) [121]. Some systems, e.g., *Kardar-Parisi-Zhang (KPZ) equation* [122], are forced by white noise. Nonequilibrium systems exhibit directional energy transfers, e.g., forward energy transfers in 3D turbulence. In addition, nonequilibrium fields are non-Gaussian and time-dependent; and the corresponding Green's function and correlation function are frequency dependent, and they are not the same.

Field-theoretic frameworks for equilibrium and nonequilibrium systems have similarities. Most calculations attempt to derive RG flow equations for the diffusive parameter, coupling constant, and forcing amplitude (see [26, 27, 122]). In HDT, the renormalized viscosity has been computed using Yakhot-Orszag's formalism, recursive RG, and functional RG. Note, however, that the coupling constant of HDT remains unchanged under RG due to the Galilean symmetry, whereas the assumption of large-scaling forcing keeps the forcing amplitude unnormalized. The energy flux for HDT too has been computed using perturbative field theory. Apart from turbulence, there are only a handful of field theory works on the energy transfers, some of which are Bratanov et al. [123] for active turbulence, and Verma et al. [120] and Yadav et al. [124] for coarsening systems.

For nonequilibrium systems, researchers employ a generalized fluctuation-dissipation theorem. One instance of such an attempt is Eqs. (34, 35), where the

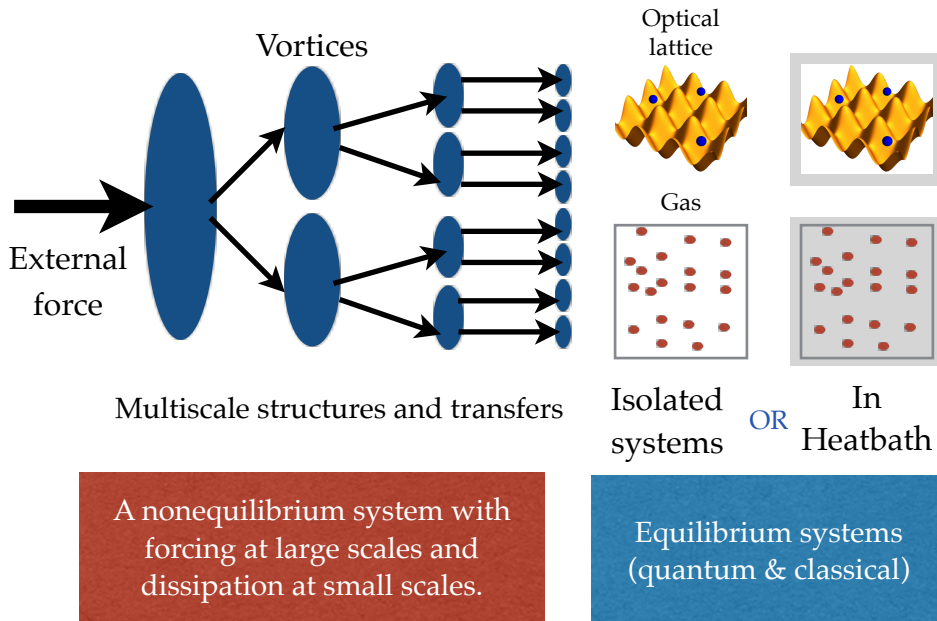


Fig. 16 Schematic diagrams of equilibrium and nonequilibrium systems. Equilibrium systems are either isolated or in contact with heat bath (shown as shaded region), whereas the nonequilibrium ones are typically forced at large scales [113]. Picture of optical lattice taken from wikipedia.

diffusion coefficient of Eqs. (200, 202) is replaced by its renormalized counterpart, $\nu(k)$. In addition, $C(\mathbf{k})$ of Eq. (35) is nonthermal, and it is derived using other means, e.g., dimensional analysis for HDT [9]. Note that Eqs. (34, 35) are phenomenological, and they have not been derived from the first principle.

The above connections among multidisciplinary field theoretic works are encouraging. Note that many field-theoretic computations of driven dissipative systems employ partial differential equations that are typically forced and dissipative. Thus, Hamiltonian or Lagrangian are not mandatory for field theory applications, contrary to a popular belief.

In Fig. 16 we contrast nonequilibrium systems with equilibrium ones. Nonequilibrium systems are typically multiscale with forcing at large scales and dissipation at small scales; this scale separation between the forcing and dissipation yields energy cascade from large scales to small scales⁵. In contrast, equilibrium systems are either isolated or in contact with heat bath, and they typically have a single scale (e.g., mean

⁵In some systems, multiple conservation laws lead to an inverse energy cascade. Two-dimensional hydrodynamics is one such example.

free path length in an ideal gas). In addition, equilibrium systems respect detailed balance and have zero energy flux, whereas nonequilibrium ones break detailed balance and exhibit nonzero energy flux.

There are several exceptions to the above classification. Three-dimensional Euler turbulence with ordered initial condition exhibits forward energy flux at large scales, but zero flux at small scales. Hence, 3D Euler turbulence is out of equilibrium at large scales and in equilibrium at small scales [5, 114, 117]. Similarly, atmospheric flows exhibit nonequilibrium behaviour at large and intermediate scales, but near-equilibrium behaviour at small scales. This is the reason why we can define local temperature for the atmosphere even when the large scales are highly dynamic.

I conclude the review in the next section.

11 Discussions and Summary

First principle calculations are rare in turbulence. Fortunately, in addition to the exact results by Kolmogorov, there are several analytical results based on field theory. In this review, I cover past works on viscosity renormalization and energy flux computations of turbulence. Starting with Kraichnan's direct interaction approximation, I discuss Yakhot-Orszag's renormalization group (RG) formalism, recursive RG by McComb and Zhou, functional RG, and RG scheme using Craya-Herring basis. In particular, the limitations and benefits of these methods are compared. For example, infrared divergence in direct interaction approximation is cured in all the RG schemes. The recursive RG scheme of McComb and Zhou is self-consistent with $k^{-5/3}$ energy spectrum, whereas the energy spectrum in Yakhot-Orszag's scheme depends on the forcing function. Another kind of perturbative field theory calculations yield the energy flux and Kolmogorov's constant for HDT. The results from these computations are consistent with numerical and experimental observations.

Note that the spectrally-truncated Euler equation ($\nu = 0$) is an isolated system that yields a very different solution. In thermalized Euler turbulence, the available Fourier modes have equal energy that yields zero energy flux [5]. However, Verma and Chatterjee [117] showed that 2D Euler turbulence does not thermalize for some ordered initial conditions.

The field-theoretic calculations of HDT have been extended to other flows, e.g., passive scalar turbulence and MHD turbulence. Note, however, that field-theoretic computation of anisotropic turbulence still remains a challenge [12, 125]. For example, we do not have successful field-theoretic calculations for stably stratified turbulence, turbulent convection, rotating turbulence, and anisotropic MHD turbulence (in the presence of a mean magnetic field). Interestingly, computation of anisotropic energy flux in weak turbulence framework is reasonably well developed [85, 86].

Field theory of turbulence share similarities with other nonequilibrium field theories, including Kardar-Parisi-Zhang (KPZ) equation [122], coarsening systems [45], and active turbulence [123]. All these computations invoke external noise, which may be thermal or nonthermal. I believe that a detailed comparison between these computations would yield interesting insights.

Phenomenologies of compressible and incompressible turbulence have significant differences. For example, shock-dominated compressible flows exhibit k^{-2} energy spectrum, rather than $k^{-5/3}$ spectrum. Interestingly, superfluid turbulence has a strong connection with compressible turbulence. Unfortunately, there are only a limited number of field-theoretic works on compressible and superfluid turbulence [126]. It is hoped that such computations would be performed in future.

Acknowledgements: The author thanks Srinivas Raghu, Pankaj Mishra, and J. K. Bhattacharjee for useful discussions. He received valuable ideas during the discussion meeting *Field Theory and Turbulence* hosted by International Centre for Theoretical Studies, Bengaluru. This work is supported by J. C. Bose Fellowship (Grant No. SERB/PHY/2023488), and by the Science and Engineering Research Board, India (Grant numbers: SERB/PHY/20215225 and SERB/PHY/2021473).

References

- [1] Peskin, M.E., Schroeder, D.V.: An Introduction To Quantum Field Theory. The Perseus Books Group, Reading, MA (1995)
- [2] Goldenfeld, N.: Lectures on Phase Transitions and the Renormalization Group. CRC Press, Boca Raton, FL (1992)
- [3] Fradkin, E.: Quantum Field Theory: an Integrated Approach. Princeton University Press, Princeton (2021)
- [4] Wilson, K.G., Kogut, J.: The renormalization group and the ε expansion. Phys. Rep. **12**(2), 75–199 (1974)
- [5] Cichowlas, C., Bonaiti, P., Debbasch, F., Brachet, M.E.: Effective Dissipation and Turbulence in Spectrally Truncated Euler Flows. Phys. Rev. Lett. **95**, 264502 (2005)
- [6] Kolmogorov, A.N.: The local structure of turbulence in incompressible viscous fluid for very large Reynolds numbers. Dokl Acad Nauk SSSR **30**, 301–305 (1941)
- [7] Kolmogorov, A.N.: Dissipation of Energy in Locally Isotropic Turbulence. Dokl Acad Nauk SSSR **32**, 16–18 (1941)
- [8] Lesieur, M.: Turbulence in Fluids. Springer, Dordrecht (2008)
- [9] Leslie, D.C.: Developments in the Theory of Turbulence. Clarendon Press, Oxford (1973)
- [10] McComb, W.D.: The Physics of Fluid Turbulence. Clarendon Press, Oxford (1990)

- [11] McComb, W.D.: *Homogeneous, Isotropic Turbulence: Phenomenology, Renormalization and Statistical Closures*. Oxford University Press, Oxford (2014)
- [12] Sagaut, P., Cambon, C.: *Homogeneous Turbulence Dynamics*, 2nd edn. Cambridge University Press, Cambridge (2018)
- [13] Orszag, S.A.: Lectures on the statistical theory of turbulence in fluid dynamics. In: Balian, R., Peube, J.L. (eds.) *Les Houches Summer School of Theoretical Physics*, p. 235. Gordon Breach, New York (1973)
- [14] Kraichnan, R.H., Montgomery, D.C.: Two-dimensional turbulence. *Rep. Prog. Phys.* **43**(5), 547–619 (1980)
- [15] Zhou, Y., Vahala, G., McComb, W.D.: *Renormalization Group (RG) in Turbulence: Historical and Comparative Perspective*. Technical Report ICAS-97-36 (1997)
- [16] Zhou, Y.: Renormalization group theory for fluid and plasma turbulence. *Phys. Rep.* **488**(1), 1–49 (2010)
- [17] Zhou, Y.: Turbulence theories and statistical closure approaches. *Phys. Rep.* **935**, 1–117 (2021) <https://doi.org/10.1016/j.physrep.2021.07.001>
- [18] Eyink, G.L., Sreenivasan, K.R.: Onsager and the theory of hydrodynamic turbulence. *Rev. Mod. Phys.* **78**(1), 87–135 (2006)
- [19] Antonov, N.V., Hnatič, M., Honkonen, J., Kakin, P.I., Lučivjanský, T., Mižišin, L.: Renormalized field theory for non-equilibrium systems. *La Rivista del Nuovo Cimento*, 1–76 (2025) <https://doi.org/10.1007/s40766-025-00064-5>
- [20] Frisch, U.: *Turbulence: The Legacy of A. N. Kolmogorov*. Cambridge University Press, Cambridge (1995)
- [21] Kraichnan, R.H.: The structure of isotropic turbulence at very high Reynolds numbers. *J. Fluid Mech.* **5**, 497–543 (1959)
- [22] Kraichnan, R.H.: Relation between Lagrangian and Eulerian correlation times of a turbulent velocity field. *Phys. Fluids* **7**(1), 142–143 (1964)
- [23] Kraichnan, R.H.: Lagrangian-History Closure Approximation for Turbulence. *Phys. Fluids* **8**(4), 575–598 (1965)
- [24] Kraichnan, R.H.: Test-field model for inhomogeneous turbulence. *J. Fluid Mech.* **56**, 287–304 (1972)
- [25] Wyld, H.W.J.: Formulation of the theory of turbulence in an incompressible fluid. *Ann. Phys.* **14**, 143–165 (1961)

- [26] Yakhot, V., Orszag, S.A.: Renormalization group analysis of turbulence. I. Basic theory. *J. Sci. Comput.* **1**(1), 3–51 (1986)
- [27] Forster, D., Nelson, D.R., Stephen, M.J.: Long-distance and long-time properties of a randomly stirred fluid. *Phys. Rev. A* **16**, 732–749 (1977)
- [28] McComb, W.D., Watt, A.: Two-field theory of incompressible-fluid turbulence. *Phys. Rev. A* **46**(8), 4797–4812 (1992)
- [29] Zhou, Y., Vahala, G., Hossain, M.: Renormalization-group theory for the eddy viscosity in subgrid modeling. *Phys. Rev. A* **37**(7), 2590–2598 (1988)
- [30] DeDominicis, C., Martin, P.C.: Energy spectra of certain randomly-stirred fluids. *Phys. Rev. A* **19**(1), 419–432 (1979)
- [31] Martin, P.C., Siggia, E.D., Rose, H.A.: Statistical dynamics of classical systems. *Phys. Rev. A* **8**, 423–437 (1973)
- [32] Verma, M.K.: Critical dimension for hydrodynamic turbulence. *Phys. Rev. E* **110**, 035102 (2024) <https://doi.org/10.1103/PhysRevE.110.035102>
- [33] L’vov, V., Procaccia, I.: Fusion Rules in Turbulent Systems with Flux Equilibrium. *Phys. Rev. Lett.* **76**(16), 2898–2901 (1996)
- [34] Falkovich, G., Gawędzki, K., Vergassola, M.: Particles and fields in fluid turbulence. *Rev. Mod. Phys.* **73**, 913–975 (2001)
- [35] Verma, M.K.: *Energy Transfers in Fluid Flows: Multiscale and Spectral Perspectives*. Cambridge University Press, Cambridge (2019)
- [36] Craya, A.: Contribution à l’analyse de la turbulence associée à des vitesses moyennes. PhD thesis, Université de Grenoble (1958)
- [37] Herring, J.R.: Approach of axisymmetric turbulence to isotropy. *Phys. Fluids* **17**(5), 859–872 (1974)
- [38] Verma, M.K.: Insights into the Energy Transfers in Hydrodynamic Turbulence Using Field-theoretic Tools. arXiv:2309.05207 (2023)
- [39] Waleffe, F.: The nature of triad interactions in homogeneous turbulence. *Phys. Fluids A* **4**(2), 350–363 (1992)
- [40] Verma, M.K.: Statistical theory of magnetohydrodynamic turbulence: recent results. *Phys. Rep.* **401**(5), 229–380 (2004)
- [41] Verma, M.K., Bhattacharya, S., Bhattacharya, S.: Euler Turbulence and thermodynamic equilibrium . arXiv, 2004–09053 (2020)

- [42] Verma, M.K.: Introduction to Statistical Theory of Fluid Turbulence. arXiv:nlin/0510069v2 (2020)
- [43] Verma, M.K., Stepanov, R., Delache, A.: Contrasting thermodynamic and hydrodynamic entropy. *Phys. Rev. E* **110**, 055106 (2024) <https://doi.org/10.1103/PhysRevE.110.055106>
- [44] McComb, W.D., Shanmugasundaram, V.: Fluid turbulence and the renormalization group: A preliminary calculation of the eddy viscosity. *Phys. Rev. A* **28**(4), 2588–2590 (1983)
- [45] Hohenberg, P.C., Halperin, B.I.: Theory of dynamic critical phenomena. *Rev. Mod. Phys.* **49**(3), 435–479 (1977)
- [46] Verma, M.K.: Variable energy flux in turbulence. *J. Phys. A: Math. Theor.* **55**(1), 013002 (2022) <https://doi.org/10.1088/1751-8121/ac354e>
- [47] Canet, L.: Functional renormalisation group for turbulence. *J. Fluid Mech.* **950**, 1 (2022) <https://doi.org/10.1017/jfm.2022.808>
- [48] Dar, G., Verma, M.K., Eswaran, V.: Energy transfer in two-dimensional magnetohydrodynamic turbulence: formalism and numerical results. *Physica D* **157**(3), 207–225 (2001)
- [49] Nandy, M.K., Bhattacharjee, J.K.: Mode-coupling theory, dynamic scaling, and two-dimensional turbulence. *Int. J. Mod. Phys. B* **09**(09), 1081–1097 (1995)
- [50] Fournier, J.D., Frisch, U.: d-dimensional turbulence. *Phys. Rev. A* **17**(2), 747–762 (1978)
- [51] Adzhemyan, L.T., Antonov, N.V., Gol'din, P.B., Kim, T.L., Kompaniets, M.V.: Renormalization group in the infinite-dimensional turbulence: third-order results. *J. Phys. A: Math. Theor.* **41**(49), 495002 (2008) <https://doi.org/10.1088/1751-8113/41/49/495002> 0809.1289
- [52] Clark, D., Armua, A., Ho, R.D.J.G., A., B.: Critical transition to a non-chaotic regime in isotropic turbulence. *J. Fluid Mech.* **930**(A17) (2022)
- [53] Adzhemyan, L.T., Antonov, N.V., Vasiliev, A.N.: Field Theoretic Renormalization Group in Fully Developed Turbulence. CRC Press, Boca Raton, FL (1999)
- [54] Gotoh, T., Yeung, P.K.: Passive scalar transport turbulence: a computational perspective. In: Davidson, P.A., Kaneda, Y., Sreenivasan, K.R. (eds.) *Ten Chapters in Turbulence*, pp. 87–131. Cambridge University Press, Cambridge (2013)
- [55] Oboukhov, A.: Structure of the temperature field in turbulent flows. *Isv. Geogr.*

Geophys. Ser. **13**, 58–69 (1949)

- [56] Corrsin, S.: On the spectrum of isotropic temperature fluctuations in an isotropic turbulence. *J. Appl. Phys.* **22**(4), 469–473 (1951) <https://doi.org/10.1063/1.1699986>
- [57] Champagne, F., Friehe, C., Larue, J., Wynagaard, J.: Flux measurements, flux estimation techniques, and fine-scale turbulence measurements in the unstable surface layer over land. *J. Atmos. Sci.* **34**, 515–530 (1977) [https://doi.org/10.1175/1520-0469\(1977\)034\(0515:FMFETA\)2.0.CO;2](https://doi.org/10.1175/1520-0469(1977)034(0515:FMFETA)2.0.CO;2)
- [58] Sreenivasan, K.R.: On the universality of the Kolmogorov constant. *Phys. Fluids* **7**(11), 2778–2784 (1995)
- [59] Zhou, Y., Vahala, G.: Renormalization-group estimates of transport coefficients in the advection of a passive scalar by incompressible turbulence. *Phys. Rev. E* **48**(6), 4387–4398 (1993)
- [60] McComb, W., Filipiak, M., Shanmugasundaram, V.: Rederivation and further assessment of the let theory of isotropic turbulence, as applied to passive scalar convection. *J. Fluid Mech.* **245**, 279–300 (1992)
- [61] Adzhemyan, L.T., Antonov, N.V., Vasil’ev, A.N.: Renormalization group, operator product expansion, and anomalous scaling in a model of advected passive scalar. *Phys. Rev. E* **58**, 1823–1835 (1998) <https://doi.org/10.1103/PhysRevE.58.1823>
- [62] Verma, M.K.: Field theoretic calculation of scalar turbulence. *Int. J. Mod. Phys. B* **15**(26), 3419–3428 (2001)
- [63] Sreenivasan, K.R.: The passive scalar spectrum and the Obukhov-Corrsin constant. *Phys. Fluids* **8**(1), 189–196 (1996)
- [64] Bellan, P.M.: *Fundamentals of Plasma Physics*. Cambridge University Press, Cambridge (2006)
- [65] Biskamp, D.: *Nonlinear Magnetohydrodynamics*. Cambridge University Press, Cambridge (1997)
- [66] Kraichnan, R.H.: Inertial-range spectrum of hydromagnetic turbulence. *Phys. Fluids* **7**, 1385–1387 (1965)
- [67] Iroshnikov, P.S.: Turbulence of a Conducting Fluid in a Strong Magnetic Field. *Sov. Astron.* **7**, 566–571 (1964)
- [68] Dobrowolny, M., Mangeney, A., Veltri, P.: Fully developed anisotropic hydro-magnetic turbulence in interplanetary space. *Phys. Rev. Lett.* **45**, 144–147 (1980)

- [69] Marsch, E.: Turbulence in the Solar Wind. In: Klare, G. (ed.) *Reviews in Modern Astronomy*, pp. 145–156. Springer, Berlin, Heidelberg (1991)
- [70] Verma, M.K., Roberts, D.A., Goldstein, M.L., Ghosh, S., Stribling, W.T.: A numerical study of the nonlinear cascade of energy in magnetohydrodynamic turbulence. *J. Geophys. Res.-Space* **101**(A10), 21619–21625 (1996)
- [71] Goldstein, M.L., Roberts, D.A.: Magnetohydrodynamic turbulence in the solar wind. *Annu. Rev. Astron. Astrophys.* **33**, 283–325 (1995)
- [72] Schekochihin, A.A.: MHD turbulence: a biased review. *J. Plasma Phys.* **88**(5), 155880501 (2022)
- [73] Mason, J., Cattaneo, F., Boldyrev, S.: Dynamic Alignment in Driven Magnetohydrodynamic Turbulence. *Phys. Rev. Lett.* **97**(25), 255002 (2006)
- [74] Biskamp, D., Müller, W.-C.: Scaling properties of three-dimensional isotropic magnetohydrodynamic turbulence. *Phys. Plasmas* **7**(12), 4889–4900 (2000)
- [75] Beresnyak, A.: Spectral Slope and Kolmogorov Constant of MHD Turbulence. *Phys. Rev. Lett.* **106**(7), 075001 (2011)
- [76] Fournier, J.-D., Sulem, P.-L., Pouquet, A.: Infrared properties of forced magnetohydrodynamic turbulence. *J. Phys. A: Math. Theor.* **15**(4), 1393–1420 (1982) <https://doi.org/10.1088/0305-4470/15/4/037>
- [77] Adzhemyan, L.T., Gratch, M., Vasil’ev, A.N.: Quantum-field renormalization group in the theory of turbulence: magnetohydrodynamics. *Theor. Math. Phys.* **64**, 777–784 (1986)
- [78] Goldreich, P., Sridhar, S.: Toward a theory of interstellar turbulence. 2: Strong alfvénic turbulence. *ApJ* **463**, 763–775 (1995)
- [79] Verma, M.K.: Field theoretic calculation of renormalized viscosity, renormalized resistivity, and energy fluxes of magnetohydrodynamic turbulence. *Phys. Rev. E* **64**(2), 026305 (2001)
- [80] Verma, M.K.: Mean magnetic field renormalization and Kolmogorov’s energy spectrum in magnetohydrodynamic turbulence. *Phys. Plasmas* **6**(5), 1455–1460 (1999)
- [81] Verma, M.K.: Field theoretic calculation of energy cascade rates in non-helical magnetohydrodynamic turbulence. *Pramana-J. Phys.* **61**(3), 577–594 (2003)
- [82] Verma, M.K.: Energy fluxes in helical magnetohydrodynamics and dynamo action. *Pramana-J. Phys.* **61**(4), 707–724 (2003)
- [83] Mizerski, K.A.: Renormalization group analysis of the magnetohydrodynamic

- turbulence and dynamo. *J. Fluid Mech.* **926**, 13 (2021) <https://doi.org/10.1017/jfm.2021.707>
- [84] Stribling, T., Matthaeus, W.H.: Relaxation processes in a low-order three-dimensional magnetohydrodynamics model. *Phys. Fluids B* **3**, 1848–1864 (1991)
- [85] Zakharov, V.E., Falkovich, G., Falkovich, G.: *Kolmogorov Spectra of Turbulence I*. Springer, Berlin Heidelberg (1992)
- [86] Nazarenko, S.V.: *Wave Turbulence*. Springer, Berlin (2011)
- [87] Rosenhaus, V., Smolkin, M.: Feynman rules for forced wave turbulence. *arXiv:2203.08168* (2023)
- [88] Barenghi, C.F., Skrbek, L., Sreenivasan, K.R.: Introduction to quantum turbulence. *PNAS* **111** *Suppl 1*, 4647 (2014)
- [89] Galtier, S., Nazarenko, S.V., Newell, A.C., Pouquet, A.G.: A weak turbulence theory for incompressible magnetohydrodynamics. *J. Plasma Phys.* **63**, 447–488 (2000)
- [90] Kraichnan, R.H.: Kolmogorov’s Hypotheses and Eulerian Turbulence Theory. *Phys. Fluids* **7**(11), 1723–1734 (1964)
- [91] Verma, M.K., Kumar, A., Gupta, A.: Hydrodynamic Turbulence: Sweeping Effect and Taylor’s Hypothesis via Correlation Function. *Trans Indian Natl. Acad. Eng.* **5**, 649 (2020)
- [92] He, G., Jin, G., Yang, Y.: Space-Time Correlations and Dynamic Coupling in Turbulent Flows. *Annu. Rev. Fluid Mech.* **49**, 51–70 (2017)
- [93] Wilczek, M., Narita, Y.: Wave-number–frequency spectrum for turbulence from a random sweeping hypothesis with mean flow. *Phys. Rev. E* **86**(6), 066308 (2012)
- [94] Taylor, G.I.: The spectrum of turbulence. *Proc. R. Soc. A* **164**(9), 476–490 (1938)
- [95] Frisch, U., Sulem, P.-L., Nelkin, M.: A simple dynamical model of intermittent fully developed turbulence. *J. Fluid Mech.* **87**(4), 719–736 (1978)
- [96] Kolmogorov, A.N.: A refinement of previous hypotheses concerning the local structure of turbulence in a viscous incompressible fluid at high Reynolds number. *J. Fluid Mech.* **13**, 82–85 (1962)
- [97] Meneveau, C., Sreenivasan, K.R.: Simple multifractal cascade model for fully developed turbulence. *Phys. Rev. Lett.* **59**(13), 1424–1427 (1987)

- [98] She, Z.-S., Leveque, E.: Universal scaling laws in fully developed turbulence. *Phys. Rev. Lett.* **72**(3), 336–339 (1994)
- [99] Belinicher, V.I., L’vov, V., Pomyalov, A., Procaccia, I.: Computing the Scaling Exponents in Fluid Turbulence from First Principles: Demonstration of Multiscaling. *J. Stat. Phys.* **93**(3/4), 797–832 (1998)
- [100] L’vov, V., Procaccia, I.: Exact resummations in the theory of hydrodynamic turbulence. I. The ball of locality and normal scaling. *Phys. Rev. E* **52**(4), 3840–3857 (1995)
- [101] L’vov, V., Procaccia, I.: Exact resummations in the theory of hydrodynamic turbulence. II. A ladder to anomalous scaling. *Phys. Rev. E* **52**(4), 3858–3875 (1995)
- [102] L’vov, V., Procaccia, I.: Exact resummations in the theory of hydrodynamic turbulence. III. Scenarios for anomalous scaling and intermittency. *Phys. Rev. E* **53**(4), 3468–3490 (1996)
- [103] Fairhall, A.L., Dhruva, B., L’vov, V.S., Procaccia, I., Sreenivasan, K.R.: Fusion rules in navier-stokes turbulence: first experimental tests. *Phys. Rev. Lett.* **79**(17), 3174–3177 (1997)
- [104] Onsager, L.: Statistical hydrodynamics. *Il Nuovo Cimento* **6**(2), 279–287 (1949)
- [105] Migdal, A.: Statistical equilibrium of circulating fluids. *Phys. Rep.* **1011**, 1–117 (2023)
- [106] Luo, G., Hou, T.Y.: Potentially singular solutions of the 3d axisymmetric euler equations. *PNAS* **111**(36), 12968–12973 (2014) <https://doi.org/10.1073/pnas.1405238111>
- [107] Eyink, G.L.: Cascades and dissipative anomalies in nearly collisionless plasma turbulence. *Phys. Rev. X* **8**, 041020 (2018) <https://doi.org/10.1103/PhysRevX.8.041020>
- [108] Moriconi, L.: Statistics of intense turbulent vorticity events. *Phys. Rev. E* **70**, 025302 (2004)
- [109] Das, A., Bhattacharjee, J.K.: Log normal intermittency and randomly stirred fluids. *EPL* **26**, 527–532 (1994)
- [110] Srednicki, M.: Chaos and quantum thermalization. *Phys. Rev. E* **50**(2), 888–901 (1994-08-01) <https://doi.org/10.1103/physreve.50.888>
- [111] Barenghi, C.F., Parker, N.G.: A primer on quantum fluids. arXiv:1605.09580 (2016)

- [112] Berry, M.V.: In: MacKay, R.S., Meiss, J.D. (eds.) Regular and irregular motion, pp. 27–53. CRC Press, New York (2020)
- [113] Verma, M.K.: Asymmetric energy transfers in driven nonequilibrium systems and arrow of time. *Eur. Phys. J. B* **92**, 190 (2019)
- [114] Verma, M.K.: Macroscopic arrow of time from multiscale perspectives. *EPL*, 21001 (2025)
- [115] Abanin, D.A., Altman, E., Bloch, I., Serbyn, M.: Colloquium: Many-body localization, thermalization, and entanglement. *Rev. Mod. Phys.* **91**(2), 021001 (2019) <https://doi.org/10.1103/revmodphys.91.021001>
- [116] Sacha, K., Zakrzewski, J.: Time crystals: a review. *Rep. Prog. Phys.* **81**(1), 016401 (2017) <https://doi.org/10.1088/1361-6633/aa8b38>
- [117] Verma, M.K., Chatterjee, S.: Hydrodynamic Entropy and Emergence of Order in Two-dimensional Euler Turbulence. *Phys. Rev. Fluids* **7**, 114608 (2022)
- [118] Pathria: *Statistical Mechanics*, 3rd edn. Elsevier, Oxford (2011)
- [119] Alert, R., Casademunt, J., Joanny, J.-F.: Active Turbulence. *Annu. Rev. Condens. Matter Phys.* **13**(1), 1–28 (2021) <https://doi.org/10.1146/annurev-conmatphys-082321-035957>
- [120] Verma, M.K., Agrawal, R., Yadav, P.K., Puri, S.: Nonlinear energy dissipation and transfers in coarsening systems. *Phys. Rev. E* **107**(3), 034207 (2023) <https://doi.org/10.1103/physreve.107.034207>
- [121] Madeira, L., Caracanhas, M.A., Santos, F.E.A., Bagnato, V.S.: Quantum turbulence in quantum gases. *Annu. Rev. Condens. Matter Phys.* **11**, 37–56 (2020)
- [122] Kardar, M., Parisi, G., Zhang, Y.-C.: Dynamic scaling of growing interfaces. *Phys. Rev. Lett.* **56**(9), 889–892 (1986) <https://doi.org/10.1103/physrevlett.56.889>
- [123] Bratanov, V., Jenko, F., Frey, E.: New class of turbulence in active fluids. *PNAS* **112**(49), 15048–15053 (2015) <https://doi.org/10.1073/pnas.1509304112>
- [124] Yadav, P.K., Verma, M.K., Puri, S.: Spectral energy transfers in domain growth problems. *Phys. Rev. E* **110**(4), 044130 (2024) <https://doi.org/10.1103/physreve.110.044130>
- [125] Alexakis, A., Biferale, L.: Cascades and transitions in turbulent flows. *Phys. Rep.* **767–769**, 1–101 (2018)
- [126] Schmitt, A.: Introduction to superfluidity. *Lect. Notes Phys* **888** (2015)